The *Legionella pneumophila* metaeffector Lpg2505 (SusF) regulates SidI-mediated translation inhibition and GDP-dependent glycosyltransferase activity

Ashley M. Joseph[1], Adrienne E. Pohl[1], Theodore J. Ball[1], Troy G. Abram[2], David K. Johnson[3], Brian V. Geisbrecht[2] and Stephanie R. Shames[1]*

[1]Division of Biology, [2]Department of Biochemistry and Molecular Biophysics, Kansas State University, Manhattan KS 66506

[3]Molecular Graphics and Modeling Laboratory, Computational Chemical Biology Core, University of Kansas, Lawrence KS 66047

*Corresponding author: Stephanie R. Shames, sshames@ksu.edu, Phone: (785) 532-0110

Running title: Metaeffector-mediated regulation of SidI function

Key words: Dot/Icm effector, SidI, *Legionella pneumophila*, metaeffector, glycosyltransferase, eEF1A

Abstract

Legionella pneumophila, the etiological agent of Legionnaires Disease, employs an arsenal of hundreds of Dot/Icm-translocated effector proteins to facilitate replication within eukaryotic phagocytes. Several effectors, called metaeffectors, function regulate the activity of other Dot/Icm-translocated effectors during infection. The metaeffector Lpg2505 is essential for *L. pneumophila* intracellular replication only when its cognate effector, SidI, is present. SidI is a cytotoxic effector that interacts with the host translation factor eEF1A and potently inhibits eukaryotic protein translation by an unknown mechanism. Here, we evaluated the impact of Lpg2505 on SidI-mediated phenotypes and investigated the mechanism of SidI function. We determined that Lpg2505 binds with nanomolar affinity to SidI and suppresses SidI-mediated inhibition of protein translation. SidI binding to eEF1A and SusF is not mutually exclusive and these proteins bind distinct regions of SidI. We also discovered that SidI possesses GDP-dependent glycosyltransferase activity and that this activity is regulated by Lpg2505. We have therefore renamed Lpg2505, SusF (suppressor of SidI function). This work reveals novel enzymatic activity for SidI and provides insight into how intracellular replication of *L. pneumophila* is regulated by a metaeffector.

Introduction

Legionella pneumophila is the etiological agent of Legionnaires' Disease, a severe inflammatory pneumonia that results from uncontrolled bacterial replication within alveolar macrophages. Upon phagocytosis, *L. pneumophila* avoids lysosomal degradation through

40 establishment of an endoplasmic reticulum-derived compartment called the *Legionella*-containing
41 vacuole (LCV) (1). For biogenesis of the LCV and acquisition of nutrients from the host cell, *L.*
42 *pneumophila* is dependent on a massive arsenal of over 300 individual effector proteins that are
43 translocated directly into the host cell through a Dot/Icm Type IVB secretion system (T4BSS) (2).
44 The cellular functions of the majority of effectors have yet to be elucidated, due in part to their
45 functional redundancy within macrophages (3).

46 Metaeffectors have emerged as a common theme in *L. pneumophila* pathogenesis and are
47 used by *L. pneumophila* to regulate effector function (4). The first metaeffector described was LubX,
48 which temporally regulates function of its cognate effector SidH by hijacking host ubiquitination
49 machinery to facilitate proteasomal degradation of SidH (5). At least 20 of the over 300 identified
50 *L. pneumophila* effectors are metaeffectors (4) and two of these – SidJ and Lpg2505 – are members
51 of a small group of effectors that are individually important for *L. pneumophila* intracellular
52 replication within macrophages (6–8). SidJ is a glutamylase that covalently modifies and
53 abrogates the function of the SidE family of effector ubiquitin ligases (9–11). Lpg2505 is a
54 metaeffector of unknown function that suppresses toxicity of its cognate effector, SidI (Lpg2504),
55 and is important for intracellular replication only when wild-type *sidI* is expressed (6). This was
56 demonstrated by restoration of *L. pneumophila* Δ*lpg2505* intracellular replication upon either
57 deletion of *sidI* or expression of a non-toxic *sidI* allele (R453P). It was further found that Lpg2505
58 was sufficient to suppress SidI-mediated toxicity towards the yeast *Saccharomyces cerevisiae* (6).
59 Thus, SidI activity is deleterious to *L. pneumophila* in the absence of Lpg2505, a unique phenotype
60 for a translocated effector.

SidI is one of seven cytotoxic *L. pneumophila* effector proteins that inhibit host cell protein translation (12). Like the majority of *L. pneumophila* effectors, *sidI* alone is dispensable for intracellular replication within macrophages, likely due to functional redundancy with other effectors (12). Other translation inhibiting effectors include Lgt1-3, SidL, LegK4, and Lpg1489 (12–16). Lgt1-3 are glycosyltransferases that inhibit translation by glucosylating eukaryotic elongation factor 1A (eEF1A) at Ser-53 (17–19). LegK4 is an effector kinase that phosphorylates heat-shock protein 70 (Hsp70), thereby reducing its ATPase activity and protein refolding activities (16). SidL and Lpg1489 have been experimentally demonstrated to inhibit host protein synthesis (13, 15), but their modes of action are unknown. Like Lgt1-3, SidI also interacts with eEF1A; however, this interaction is insufficient for translation inhibition (12). SidI also interacts with eEF1Bγ and induces the host heat shock response (12). To date, the mechanism(s) by which SidI functions within the host cell to inhibit host protein synthesis have not been elucidated.

In this study we aimed to discern how Lpg2505 regulates SidI and gain insight into the molecular mechanism of SidI function. We discovered that Lpg2505 and SidI bind with nanomolar affinity and that Lpg2505 suppresses SidI-mediated translation inhibition *in vitro.* Furthermore, SidI interaction with Lpg2505 and eEF1A are not mutually exclusive and these two proteins bind with distinct regions of SidI. Finally, we discovered novel GDP-dependent glycosyltransferase activity for SidI, which is regulated by Lpg2505. For this reason, we have named Lpg2505 as *suppressor of SidI function* (SusF).

Results

SusF and SidI bind with nanomolar affinity.

Lpg2505 (SusF) is sufficient to suppress SidI-mediated cytotoxicity and promote *L. pneumophila* intracellular replication (6). To reveal a potential mechanism for SusF-mediated regulation of SidI, we evaluated whether SusF interacts with SidI. Since effectors function within host cells, we investigated whether SidI and SusF interact in the presence of host cell lysates. HEK 293 cells stably producing 3FLAG-eipotpe tagged SusF were generated and we initially attempted to ectopically express GFP-tagged *sidI* within these cells for co-immunoprecipitation. However, wild-type SidI could not be detected, likely due to potent translation inhibition. Thus, we generated recombinant GST-tagged SidI (GST-SidI) and evaluated its ability to interact with 3FLAG-SusF within HEK 293 lysates (see *Materials and Methods*). We found that GST-SidI, but not GST alone, retained 3FLAG-SusF on glutathione-coated beads (**Fig 1A**). Furthermore, GST-SidI - but not GST alone - was retained on Ni-NTA beads coated with recombinant His_6-SusF (**Fig 1B**). Thus, SusF interacts with SidI in the presence or absence of mammalian cell lysates.

To determine if SidI and SusF bind directly, we examined the ability of these proteins to associate with one another throughout the course of sequential column chromatography procedures. SidI and SusF were co-expressed in *Escherichia coli*, purified by Ni-NTA affinity chromatography (see *Materials and Methods*), and the eluted proteins were separated by analytical format size exclusion chromatography. We found that SidI and SusF co-eluted from the column as a species corresponding to a molecular weight of ~150 kDa, as judged by comparison to a panel of known protein standards (**Fig 1C**). Bands corresponding to both proteins were detected in samples of

column fractions that had been separated by SDS-PAGE and analyzed by Coomassie staining (**Fig S1**). Thus, SidI and SusF interact directly and appeared to form a stable complex.

We subsequently used surface plasmon resonance (SPR) to investigate the affinity and kinetics of the SusF-SidI interaction. We immobilized SusF on an SPR surface using random amine chemistry and injected recombinant, purified SidI at increasing concentrations. We employed a single-cycle approach due to difficulty with regenerating the SusF surface following exposure to SidI. We found that the reference-corrected sensorgram could be described fairly well by a Langmuir binding model (K_D = 0.89 nM and χ^2 = 3.26) (**Fig. S2**), but was better fit to a two-state reaction model (K_D = 3.1 nM and χ^2 = 0.79) (**Fig 1D**). A particularly noteworthy feature of the SusF-SidI interaction is its long half-life, with an estimate dissociation rate constant between 2-5x10^{-4} s^{-1}. This observation explains, at least in part, the ability of SusF and SidI to remain associated with one another throughout the co-purification procedures described above. Taken together, these data indicate that SusF binds directly to SidI and forms a high-affinity complex with a K_D of ~ 1 nM.

SusF suppresses SidI-mediated translation inhibition.

Based on the high-affinity interaction between SidI and SusF, we hypothesized that SusF represses SidI-mediated translation inhibition. To test this hypothesis, we quantified translation of *Firefly* luciferase mRNA (Luc mRNA) *in vitro* (see *Materials and Methods*). This assay was used previously to demonstrate that ≥ 5 ng of recombinant SidI was sufficient to completely abolish translation (12). We confirmed that purified His_6-SidI significantly attenuates protein translation

and additionally revealed that purified SusF alone has no impact on translation (**Fig 2A**). We further determined that SusF significantly rescues translation in the presence of SidI (P<0.01, **Fig 2B**). Thus, SusF is sufficient to suppress SidI-mediated translation inhibition *in vitro.*

Our SPR data demonstrates that the SidI-SusF interaction occurs rapidly. We therefore hypothesized that pre-formation of the SidI-SusF complex would not result in further attenuation of SidI-mediated translation inhibition. To determine whether or not pre-formation of the SidI-SusF complex would enhance SusF-mediated suppression of translation inhibition, we incubated SidI with SusF for 30 min prior to addition to the *in vitro* translation reaction. Pre-formation of the SidI-SusF complex did not further attenuate SidI-mediated translation inhibition (**Fig 2C**; see *Materials and Methods*). Furthermore, SusF was insufficient to reverse SidI-mediated translation inhibition since addition of SusF to the reaction after either 30 min or 60 min did not restore translation (**Fig 2C**). Finally, we evaluated whether suppression of SidI-mediated translation inhibition by SusF was dose dependent. SusF was added in concentrations ranging from equimolar up to a 15-fold molar excess relative to SidI. An equimolar amount of SusF was sufficient to suppress SidI-mediated translation inhibition and translation was not further enhanced by addition of up to a 15-fold molar excess of SusF (**Fig 2D**). Thus, equimolar amounts of SusF are sufficient to suppresses SidI-mediated translation inhibition.

SusF does not affect the interaction between SidI and eEF1A.

A previous report demonstrated that SidI interacts directly with the transcription factor eukaryotic elongation factor 1A (eEF1A) (12). We therefore investigated whether the interactions

144 between SidI and eEF1A or SusF are mutually exclusive. GST-SusF or GST alone were
145 immobilized on glutathione beads and incubated with His_6-SidI that was pre-incubated with
146 HEK 293T lysates. We found that eEF1A was retained on the beads only in the presence of SidI
147 and that eEF1A did not impair interaction between SusF and SidI (**Fig 3A**). Subsequently, we
148 asked whether increasing the concentration of SusF would influence the SidI-eEF1A interaction.
149 We incubated GST-SidI with eEF1A (from HEK 293T lysates, see *Materials and Methods*) followed
150 by increasing concentrations of purified recombinant SusF. Despite SusF concentration increasing
151 100-fold, GST-SidI still retained eEF1A on the beads (**Fig 3B)**, suggesting that SidI interacts with
152 SusF and eEF1A simultaneously. The same result was observed when SusF was incubated with
153 GST-SidI prior to HEK 293T lysates (**Fig S3**). Thus, SidI binding to eEF1A and SusF is not
154 mutually exclusive.

155

156 ***SusF and eEF1A interact with distinct regions of SidI.***

157 Since both SusF and eEF1A are capable of binding SidI simultaneously, we hypothesized that
158 these proteins interact with SidI at distinct sites. SidI has a molecular weight of ~ 110 kDa and
159 consists of 942 amino acids. Since the structure of SidI has not been solved, we used the RaptorX
160 webserver (20) to predict the domain structure of SidI. Based on the predicted domains (**Fig S4**),
161 we generated SidI truncations consisting of amino acid residues 1-268 ($SidI_N$), 269-942 ($SidI_C$) and
162 269-874 ($SidI_{C\Delta 68}$) (**Fig 4A**). To determine which of these putative SidI domains is involved in
163 interaction with SusF and eEF1A, we immobilized GST-tagged full-length SidI, $SidI_N$, $SidI_C$,
164 $SidI_{C\Delta 68}$, or GST alone on glutathione beads followed by incubation with lysates from HEK 293

cells stably producing 3FLAG-SusF. Western blot analysis was used to detect 3FLAG-SusF and eEF1A bound to SidI truncation proteins (see *Materials and Methods*). We confirmed that GST-SidI, but not GST alone, was capable of retaining both SusF and eEF1A on the beads. 3FLAG-SusF was further retained on beads coated with GST-SidI$_N$ and GST-SidI$_C$ but not GST-SidI$_{C\Delta 68}$, whereas eEF1A was retained by GST-SidI$_C$ and GST-SidI$_{C\Delta 68}$ (**Fig 4B**). To control for the potential influence of 3FLAG-SusF on eEF1A binding to SidI, we repeated this experiment using HEK 293 cells that do not express *3FLAG-susF*. We observed the same pattern of interactions between eEF1A and the C-terminal region of SidI in the absence of 3FLAG-SusF (**Fig S5**). Based on these data, we conclude that SusF interacts with SidI at regions within amino acid residues 1-268 and 874-942 whereas eEF1A interaction with SidI is dependent on amino acid residues 269-874. Together, these data suggest SusF interacts with two regions of SidI that are distinct from the site of SidI interaction with eEF1A.

SidI is not dependent on SusF for translocation into host cells.

The majority of *L. pneumophila* effector proteins rely on a C-terminal translocation signal for Dot/Icm-mediated translocation into host cells (21, 22). Based on the observed interaction between SusF and the C-terminal 68 amino acid residues of SidI, we hypothesized that SusF may impact Dot/Icm-mediated translocation of SidI. To test this hypothesis, we quantified the export of SidI fused to *Bordetella pertussis* adenylate cyclase (CyaA) (21). When CyaA fusion proteins reach the cytosol of eukaryotic cells they catalyze formation of cAMP, which can be quantified using cAMP-specific ELISA. Based on potent toxicity associated with wild-type SidI, a non-toxic

186 *sidI* allele (R453P; SidI$_{RP}$) was used for these experiments (6, 12). Expression of CyaA-SusF and
187 CyaA-SidI$_{RP}$ was confirmed using Western blot analysis (**Fig 5A**). Subsequently, we found that
188 cAMP production by host cells was significantly increased following infection with wild-type
189 and Δ*susF*, but not Δ*dotA*, strains of *L. pneumophila* producing CyaA-SidI$_{RP}$ (**Fig 5B**). Translocation
190 of CyaA-RalF was used as a positive control for Dot/Icm-dependent translocation (21) (**Fig 5A,**
191 **B**). Together, these data demonstrate that SidI is not dependent on SusF for translocation into
192 host cells.

193

194 ***Binding to eEF1A is insufficient for SidI-mediated translation inhibition.***

195 Subsequently, we investigated the ability of truncated SidI proteins to influence protein
196 translation. At concentrations equivalent to SidI, neither SidI$_{N}$ nor SidI$_{CΔ68}$ were sufficient to
197 inhibit protein translation *in vitro* (**Fig 6A**). Based on the interaction between SidI$_{CΔ68}$ and eEF1A,
198 we also quantified translation in the presence of increasing concentrations of His$_6$-SidI$_{CΔ68}$. We
199 found that His$_6$-SidI$_{CΔ68}$ significantly decreased translation at concentrations up to 25-fold greater
200 than SidI (**Fig 6B**), suggesting that this truncation retains some activity; however, SidI$_{CΔ68}$-
201 mediated translation inhibition is modest in comparison to an equal amount of SidI despite the
202 ability to interact with eEF1A (**Fig 4B**, **Fig S5**). These data further confirm that interaction with
203 eEF1A is insufficient for SidI-mediated translation inhibition (12).

204

205 ***SidI is a GDP-dependent glycosyltransferase.***

Like many other bacterial effectors, the primary amino acid sequence of SidI does not have obviously conserved motifs. Therefore, to gain insight into the putative function of SidI, we used a variety of computational methods to predict the structure and function of SidI. Though very low primary sequence identity was present in the templates used, the HHPred webserver (23), the Phyre2 webserver (24), the Raptor-X webserver (20), and the I-TASSER webserver (25–27) all produced models of various lengths, but with the same fold for overlapping regions. A DALI search (28) for structural homologs against each of these models revealed that amino acid residues 368-868 of SidI have predicted structural homology to multiple bacterial and eukaryotic glycosyltransferases with GT-B folds, including PimB, a GDP-mannose-dependent mannosyltransferase (**Table S1, Fig S6**). Orthogonally, the Ginzu domain parser on the Robetta server also predicted the presence of a glycosyltransferase domain (29). Based on the consensus between orthogonal computational approaches, we hypothesized that SidI possesses GDP-dependent glycosyltransferase activity and that GDP-mannose could be a substrate. To test this hypothesis, we utilized a functional luminescence-based assay to quantify cleavage of GDP-mannose (see *Materials and Methods*). As a control, we also evaluated the ability of SusF, which does not have predicted glycosyltransferase activity, to cleave GDP-mannose. We observed high levels of free GDP only following incubation of recombinant His_6-SidI with GDP-mannose, suggesting that SidI indeed possesses GDP-dependent glycosyltransferase activity (**Fig 7A**). We further investigated whether SidI glycosyltransferase activity was specific to GDP-sugars and evaluated its ability to cleave UDP-glucose, which is cleaved by Lgt1-3 (18, 30). SidI was capable of cleaving UDP-glucose, but far less efficiently than GDP-mannose (**Fig 7B**), suggesting that

GDP-mannose is the preferred substrate. Together, these data suggest that SidI functions specifically as a GDP-dependent glycosyltransferase.

The entire predicted GDP-dependent glycosyltransferase domain of SidI is encoded by amino acids 350-874, which is encompassed within SidI$_{C\Delta 68}$ truncation (**Fig 4A**). To determine whether SidI$_{C\Delta 68}$ alone is sufficient to cleave GDP-mannose, we incubated His$_6$-SidI$_{C\Delta 68}$ with GDP-mannose and quantified generation of free GDP. Full-length SidI and SidI$_N$, which is not predicted to possess glycosyltransferase activity, were included as controls. Neither SidI$_N$ nor SidI$_{C\Delta 68}$ were sufficient to cleave GDP-mannose (**Fig 7C**), suggesting that SidI enzymatic activity is dependent on both the N- and C-terminal domains.

SidI enzymatic activity is dampened by SusF

Based on the ability of SusF to suppress SidI-mediated translation inhibition, we hypothesized that SusF could regulate SidI-mediated GDP-dependent glycosyltransferase activity. Thus, SidI-mediated GDP-mannose cleavage in the presence of equimolar amounts of SusF was quantified as above. We found that SusF was sufficient to significantly decrease – but not inhibit – SidI GDP-dependent glycosyltransferase activity (**$P < 0.01$, **Fig 7D**). We further evaluated whether addition of molar excess of SusF would further decrease SidI glycosyltransferase activity; however, addition of up to a 5-fold molar excess of SusF to SidI was not sufficient to significantly inhibit SidI activity compared to equimolar quantities (**Fig 7E**). Thus, SusF dampens SidI glycosyltransferase activity *in vitro*.

Discussion

Legionella pneumophila is an opportunistic, intracellular pathogen that exploits host cell machinery to promote intracellular replication through the translocation of effector proteins. SidI is one of seven cytotoxic effectors that inhibit eukaryotic protein translation (SidI, SidL, Lgt1-3, LegK4, Lpg1489) (12, 13, 15, 18). Within this family of effectors, SidI is distinct as its regulation by the metaeffector Lpg2505 (SusF) is essential for intracellular replication (6). Our study aimed to explore the role of SusF in regulation of SidI function and elucidate potential mechanisms behind SidI-mediated toxicity. Here we demonstrate that SusF binds directly to SidI with high affinity and modulates both SidI-mediated translation inhibition and novel GDP-dependent glycosyltransferase activity, which has not been previously observed for a bacterial effector. We further demonstrate that SidI is able to simultaneously bind SusF and eEF1A, which interact with distinct regions of SidI. This work is the first to define the enzymatic activity of SidI and the contribution of SusF to SidI-mediated phenotypes.

L. pneumophila is reliant on the host cell-derived amino acids for intracellular replication (31). It can therefore be speculated that *L. pneumophila* utilizes multiple effector proteins to halt host protein synthesis at the elongation step in order to facilitate proteasomal degradation of partially folded polypeptides. The translation inhibiting effectors characterized to date have diverse functions. The effector Lgt1 was found to target the host elongation factor eEF1A and homology searches led to the discovery of the orthologous effectors Lgt2-3(19). The Lgt effectors function by glycosylation of eEF1A at Ser-53, which results in blockade of host protein synthesis

(32). The Lgts also glycosylate a eukaryotic release factor related protein (eRF3) and the Hsp70 subfamily B suppressor 1 (Hbs1) (33, 34). Based on the function of Lgt1-3, attempts were made to identify SidI-mediated post-translational modification of eEF1A; however, no modifications were discovered (12). Although SidI was previously assumed to lack glycosyltransferase activity (12, 35), we discovered that SidI, like the Lgts, is indeed able to cleave GDP-mannose, suggesting that SidI is a mannosyltransferase. However, future investigation is required to reveal the target of SidI's activity *in vivo* and the molecular mechanism by which SidI inhibits translation.

SidI induces the host stress response through formation of a complex between heat shock factor 1 (HSF1) and eEF1A(12). The formation of this complex in conjunction with a non-coding RNA promotes the binding of HSF1 to the heat shock element (HSE), inducing host cell *Hsp70* expression (12, 36). Notably, despite the upregulation of transcription, Hsp70 protein levels did not differ between infected and uninfected cells (12), likely due to robust translation inhibition by *L. pneumophila* effectors. A more recent study revealed that the eEF1A1 isoform facilitates expression of heat shock genes independently of its role in protein translation (37). Since SidI, but not Lgt1, induced expression of *Hsp70* in addition to eEF1A-mediated activation of the heat shock factor 1 (HSF1) transcription factor, it could be hypothesized that SidI modulates eEF1A to specifically amplify heat shock genes, which could enhance survival of *L. pneumophila* infected cells. Moreover, the effector LegK4 phosphorylates Hsp70, which results in loss of protein translation. It is tempting to envision a scenario whereby SidI and LegK4 function in concert to modulate host Hsp70 activity. The importance for modulation of heat shock proteins has also been demonstrated by previous observations that Hsp90 is essential for *L. pneumophila* replication

289 in *Acanthamoeba castellanii* (38). Further investigation is required to define the influence of SusF
290 on SidI-mediated modulation of the heat shock response.

291 Regulation of effector function by metaeffectors is an essential component of the *L.*
292 *pneumophila* virulence strategy. The first identified *L. pneumophila* metaeffector, LubX, functions
293 as an E3 ubiquitin ligase that is translocated into the host cytosol at late stages of infection and
294 catalyzes ubiquitination of the effector protein SidH, targeting it for proteasomal degradation (5).
295 *L. pneumophila* Δ*lubX* mutants replicate similarly to wild-type bacteria, suggesting that LubX is
296 not individually required for intracellular replication in host cells examined (5). Like SusF, the
297 metaeffector SidJ directly contributes to intracellular replication by suppressing the toxicity of the
298 SidE family of effectors (SdeA, SidE, SdeB and SdeC) (7, 39). However, unlike SusF,
299 overexpression of SidJ is toxic to eukaryotic cells (39). The SidE family of effectors also contributes
300 directly to intracellular replication through a novel mechanism of phosphoribosyl-ubiquitin
301 conjugation to host substrates (40–42). Unlike the SidE effectors, loss of *sidI* or the *sidI-lpg2505*
302 operon has no effect on *L. pneumophila* intracellular growth (6), suggesting that SidI functions
303 redundantly within macrophages. However, in the absence of SusF, SidI is deleterious to *L.*
304 *pneumophila* intracellular replication (6), a phenotype not observed for any other effector.

305 Several modes of metaeffector function have been described. A large-scale screen by
306 Urbanus and colleagues led to the discovery of 17 novel *L. pneumophila* metaeffectors that function
307 to suppress the toxicity of their cognate effectors (4). They uncovered several mechanisms by
308 which metaeffectors regulate their cognate effectors through abrogation of effector enzymatic
309 activity *in vitro* (LegL1, SidP, LupA). Similarly, we found that SusF dampens SidI activity *in vitro*;

however, residual SidI activity is retained, suggesting that SusF functions to fine-tune SidI activity. Although we have not identified the *bona fide* substrate of SidI, our observation that SidI interacts with both SusF and eEF1A simultaneously at distinct regions suggests that SidI may modify eEF1A or use interaction with eEF1A to gain access to a host substrate. Future investigation will reveal the role of SusF in SidI function and how this contributes to *L. pneumophila* intracellular replication.

Through structural homology prediction and biochemical analysis, we revealed that SidI likely possesses GDP-dependent glycosyltransferase activity. Although we have not directly demonstrated the transfer of mannose to a substrate protein, it is unlikely that SidI functions only as a nucleotide-sugar hydrolase in the context of infection. Moreover, detection of free nucleotide liberation from nucleotide-sugar donors is a pre-requisite for transfer of glycans to substrate molecules and is an established method to identify glycosyltransferase activity without knowing the acceptor substrate (43). Our use of a luciferase-based assay eliminates the requirement for radioactive nucleotide-sugars.

Several *L. pneumophila* effectors function as glycosyltransferases, including the translation inhibitors Lgt1-3; however, none have been shown to utilize GDP-conjugated sugars. In fact, bacterial GDP-dependent glycosyltransferases seem to be involved primarily in biogenesis of cell surface structures (44–46). SidI has predicted structural homology to mycobacterial phosphatidylinositol mannosides (PIMs), which are GT-B glycosyltransferases (45, 47). To our knowledge, no other translocated bacterial effector has been demonstrated to have GDP-dependent glycosyltransferase activity. The primary site of protein glycosylation in eukaryotic

cells is the Golgi apparatus; however, nucleotide sugars, including GDP-mannose, are synthesized in the cytoplasm of eukaryotic cells prior to transport into the Golgi (48, 49). Thus, SidI likely hijacks cytoplasmic GDP-mannose prior to its translocation into the Golgi. Based on the relatively low abundance of individual effectors in *L. pneumophila* infected cells it is unlikely that SidI function influences glycoprotein production by host cells. Thus, SidI is a GDP-dependent glycosyltransferase and this activity is likely critical for SidI-mediated translation inhibition and cytotoxicity. Further biochemical and structure-function analysis will reveal the detailed molecular mechanism by which SidI functions, its *bona fide* substrate in host cells and how SusF regulates its activity to promote *L. pneumophila* intracellular replication.

In this study, we have revealed a direct high-affinity interaction between SidI and its metaeffector SusF, defined a novel enzymatic activity for SidI and uncovered that SusF can modulate SidI function *in vitro*. Our work has provided a foundation for future biochemical and cell biological studies to reveal how SidI functions to modulate host cell processes. The severe virulence defect resulting from expression of *sidI* in the absence of *susF* underlies the importance of defining the molecular mechanism of SidI-SusF function. Moreover, the lack of precedent for a bacterial GDP-dependent glycosyltransferase effector protein suggests that SidI possesses novel enzymatic activity, which must be regulated by SusF to promote *L. pneumophila* intracellular replication. Our future work will focus on uncovering this mechanism in order to gain critical insight into translation inhibition and metaeffector function.

Materials and Methods

352 Bacterial strains, cell culture, growth conditions and reagents.

353 *Escherichia coli* stains used for cloning (Top10; Invitrogen) and protein expression [BL21 (DE3); a
354 gift from Dr. Craig Roy, Yale University] were maintained in Luria-Bertani (LB) medium
355 supplemented with antibiotics as appropriate for plasmid selection [50 μg mL^{-1} kanamycin
356 (GoldBio), 100 μg mL^{-1} ampicillin (GoldBio) and 25 μg mL^{-1} chloramphenicol (GoldBio)].
357 *Legionella pneumophila* Philadelphia-1 Lp01 (50) and Δ*dotA* (51) strains were cultured on
358 supplemented charcoal–N (2-acetamido)-2-aminoethanesulfonic acid (ACES)-buffered yeast
359 extract (CYE) and grown at 37˚C as described previously (52, 53). CYE was supplemented with
360 10 μg mL^{-1} chloramphenicol for plasmid maintenance as required. Protein expression in *E. coli*
361 and *L. pneumophila* was induced with 1 mM isopropyl-β-D-1-thiogalactopyranoside (IPTG)
362 (GoldBio).

363 All mammalian cells were grown at 37˚C/5% CO_2 for up to 30 passages. HEK 293 cells were
364 cultured in Dulbecco's Modified Eagle Medium (DMEM; Gibco) supplemented with 10% heat-
365 inactivated fetal bovine serum (HIFBS; Gibco). CHO FcγrII cells (54) (a gift from Dr. Craig Roy)
366 were cultured in MEMα (Gibco) supplemented with 10% HIFBS.

367 Unless otherwise specified, all chemicals were obtained from MilliporeSigma (St Louis, MO).
368 Oligonucleotide primers used in this study are listed in **Table 1**.

369

370 Molecular cloning, plasmid construction and generation of *Legionella* strains.

371 *Legionella pneumophila* Lp01 gDNA was isolated using the Illustra genomicPREP DNA isolation
372 spin kit (GE Healthcare) and was used as a template for cloning *sidI* and *susF* into the indicated
373 plasmid vectors. For recombinant protein production, *sidI* was amplified using primer pairs
374 SidIBamHI-F/SidINotI-F and cloned as a BamHI/NotI fragment into pGEX-6P-1 (GE Healthcare)
375 and pT7HMT (55). *susF* was amplified using primer pairs SusFBglII-F/SusFNotI-R and cloned as
376 a BglII/NotI fragment into BamHI/NotI-digested pGEX-6P-1 and pcDNA4T/O-3xFLAG (56). For
377 cloning into pT7HMT, *susF* was amplified using SusFSalI-F/SusFNotI-R primer pairs and cloned
378 as a SalI/NotI fragment. For generation of SidI truncations, the regions of interest were amplified
379 with primer pairs SidIBamHI-F/SidINNotI-R ($SidI_N$), SidICBamHI-F/SidINotI-R ($SidI_C$), or
380 SidICBamHI-F/SidICΔ68NotI-R ($SidI_{CΔ68}$) and cloned as BamHI/NotI fragments into pT7HMT or
381 pGEX-6P-1. For generation of p*cyaA*::$sidI_{RP}$, $sidI_{R453P}$ was amplified from pSR47S::$sidI_{R453P}$ (6) with
382 SidIBamHI-F2/SidIPstI-R and cloned as a BamHI/PstI fragment into p*cyaA* (21). DNA sequences
383 were confirmed by Sanger sequencing (GENEWIZ, South Plainfield, NJ).

384 *L. pneumophila* Lp01 wild-type and Δ*dotA* producing CyaA-SidI constructs were generated by
385 electroporation of p*cyaA*::$sidI_{RP}$ into competent strains using a BioRad Gene Pulser at 2.4 kV, 200
386 Ω, and 0.25 μF and plated on CYE supplemented with 10 μg mL^{-1} chloramphenicol. CyaA-SidI
387 production was confirmed by Western blot as described below. *L. pneumophila* strains harboring
388 p*cyaA*::*ralF* (21) were a gift from Dr. Craig Roy (Yale University).

389

390 <u>Transfection and selection of stable tissue culture cells</u>

391 HEK 293 cells were transfected with pcDNA4T/O-3FLAG::*susF* using FuGENE HD (Roche)
392 transfection reagent according to manufacturers' instructions. At 48 h post-transfection, cells 500
393 μg mL^{-1} zeocin (Invitrogen) was added to culture medium and this selection was maintained for
394 10 days. Subsequently, cells were maintained in 200 μg mL^{-1} zeocin and production of 3FLAG-
395 SusF was confirmed by Western blotting, as described.

396

397 Recombinant protein expression and purification

398 Overnight *E. coli* BL21 (DE3) cultures were sub-cultured at 1:100 for 3 h in LB supplemented with
399 the appropriate antibiotics followed by induction of protein expression with 1 mM IPTG, and
400 induced at 16˚C overnight. Bacterial cultures were centrifuged at 4,200 r.c.f. for 5 min at 4˚C and
401 washed with ice-cold PBS followed by incubation in bacterial lysis buffer [50 mM Tris pH 8, 100
402 mM NaCl, 1 mM ethylenediaminetetraacetic acid (EDTA), 200 μg mL^{-1} lysozyme, 2 mM
403 dithiothreitol (DTT), 10 μg mL^{-1} DNase, and complete protease inhibitor] for 30 min on ice.
404 Bacteria were sonicated on ice followed by centrifugation at 17,000 r.c.f. for 30 min at 4˚C.
405 Clarified bacterial lysates were incubated with either Ni-NTA beads plus 15 mM imidazole (His-
406 tag) or Glutathione Agarose beads (GST-tag) for 1-2 h at 4˚C with rotation. For His-tagged
407 proteins, Ni-NTA agarose beads were transferred to 10 mL polyprep chromatography columns
408 (BioRad) and washed with 20 mL of ice-cold wash buffer (50 mM Tris pH 8, 100 mM NaCl, 1 mM
409 EDTA, 40 mM imidazole) followed by elution in 7 mL of elution buffer (50 mM Tris pH 8, 100
410 mM NaCl, 1 mM EDTA, 200 mM imidazole). For GST-tagged proteins, glutathione agarose beads
411 were transferred to a 10 mL polyprep chromatography column and washed with 20 mL wash

412 buffer I (PBS, 0.05% Triton X-100), followed by wash buffer II (PBS, 0.05% Triton X-100, 0.5 M
413 NaCl) and eluted in GST elution buffer (50 mM Tris pH 9.5, 10 mM glutathione). Protein eluates
414 were visualized by SDS-PAGE and Coomassie brilliant blue staining. Elution fractions containing
415 protein were combined, dialyzed into PBS and quantified by Bradford Assay (Thermo Scientific).

416 In some cases, the poly-histidine tag was removed from recombinant proteins by site-
417 specific proteolysis using Tobacco Etch Virus protease. Following digestion as previously
418 described (55), the sample was reapplied to a Ni-NTA beads and the unbound fraction containing
419 the target protein was collected. Samples were further purified by gel filtration chromatography
420 using either a Superdex 75 (26/60) or Superdex 200 (26/60) column attached to an AKTA-format
421 FPLC (GE Healthcare) and PBS as a running buffer. Elution fractions containing protein were
422 analyzed by SDS-PAGE and Coomassie brilliant blue staining, as described above.

423

424 Affinity chromatography for protein-protein interaction

425 Overnight *E. coli* cultures grown in LB plus appropriate antibiotic were sub-cultured 1:100 into
426 20 mL LB and grown at 37˚C for 3 h followed by induction with 1 mM IPTG for 4 h. Cultures
427 were centrifuged for 10 min at 1500 r.c.f., washed with ice-cold PBS and pelleted in 1 mL aliquots
428 prior to storage at -20°C for <72 hours until use. Pellets were re-suspended in 1 mL of cold lysis
429 buffer (50 mM Tris pH 8, 100 mM NaCl, 1 mM EDTA) supplemented with 200 μg mL^{-1} lysozyme,
430 and complete protease inhibitor and incubated on ice for 30 min. Two millimolar DTT was added
431 to lysates before sonicating on ice. Lysates were then clarified by centrifugation at 12,600 r.c.f. for
432 15 min at 4˚C. Supernatants were collected in fresh, pre-chilled microcentrifuge tubes.

Supernatants were added to either pre-equilibrated Ni-NTA magnetic beads or magnetic glutathione agarose beads following manufacturer's protocol (Pierce) for binding His- or GST-tagged fusion proteins, respectively. After the initial batch binding, beads were washed 2x with wash buffer [Ni-NTA: 50 mM Na_3PO_4, 300 mM NaCl, 15 mM imidazole, 0.05% Tween-20, pH 8; Glutathione: 125 mM Tris-Cl, 150 mM NaCl, 1mM DTT, 1 mM EDTA, pH 7.4] prior to addition of recombinant protein or subsequent cell lysate and batch binding for 1 h at 4˚C with rotation. Beads were washed 2x with wash buffer before adding the final cell lysate or recombinant protein and incubating for 1 h at 4˚C with rotation. Following binding, beads were washed 2x with wash buffer and transferred to fresh, pre-chilled 1.5 mL microcentrifuge tubes and resuspended in 25 µL of 3x Laemmli sample buffer and boiled for 10 min. Samples were analyzed by SDS-PAGE and Coomassie brilliant blue or Western Blot, as indicated.

For experiments to examine eEF1A binding, lysates were derived from either HEK293T or HEK293 3FLAG-SusF cells grown to ≥70% confluence on tissue culture (TC) treated dishes. Cells were washed 1x with ice-cold PBS and lysed in 1 mL of mammalian lysis buffer [1% NP-40 (v/v), 150 mM NaCl, 20 mM Tris-Cl pH 7.5, 10 mM $Na_4P_2O_7$, 50 mM NaF, and complete protease inhibitor]. Lysates were collected in pre-chilled, 1.5 mL centrifuge tubes and centrifuged at 11,000 r.c.f. for 20 min at 4˚C. Supernatants were collected in pre-chilled, 1.5 mL centrifuge tubes and stored on ice until use.

CyaA effector translocation assay

453 Translocation of CyaA fusion proteins was performed as described (21). Briefly, CHO FcγrII cells
454 (a gift from Dr. Craig Roy) were seeded into 24-well plates at $1x10^5$ cells per well 24 h prior to
455 infection. Cells were infected at a multiplicity of infection (MOI) of 30 with *L. pneumophila* Lp01
456 wild-type or Δ*dotA* that had been cultured on CYE supplemented with 10 μg mL-1
457 chloramphenicol and 1 mM IPTG followed by opsonization by incubation for 30 min with an α-
458 *L. pneumophila* antibody (Invitrogen, PA17227; 1:1000) at RT. Cell culture media was
459 supplemented with 1 mM IPTG to ensure expression of CyaA-SidI fusion protein. Infected cells
460 were incubated for 1-2 hours at 37°C/5% CO_2 followed by aspiration of culture media and
461 washing 3 times with ice-cold PBS. Cells were lysed for 30 minutes in 200 μL of ice-cold lysis
462 buffer (50 mM HCl, 0.1% Triton-X100) with rocking at 4˚C. Samples were either stored at -80˚C
463 until use or immediately mixed with 12 μL 0.5M NaOH in 95% ethanol and centrifuged for 5 min
464 at 11,000 r.c.f. Supernatants were dried in a Speed Vac and stored at -80°C until use. cAMP was
465 quantified using a cAMP Direct Biotrak EIA (non-acetylation) kit (GE Healthcare). Briefly, dried
466 samples were resuspended in 250 μL Assay Buffer and ELISA was performed following
467 manufacturer's protocol. Absorbance at 655 nm was read in a Victor 2 microplate reader
468 (PerkinElmer).

469

470 <u>*In vitro* protein translation assay</u>

471 Translation assays were performed using the Promega Flexi® Rabbit Reticulocyte Lysate System
472 (RLL; L4540) following manufacturer's protocol. Briefly, a master mix of RLL was generated and
473 aliquoted into individual tubes. Four nanograms of purified His_6- SidI (see above) were added as

474 indicated. Purified recombinant (untagged) SusF was added at the indicated concentrations.
475 Proteins were equilibrated to room temperature before use. All reactions were brought to 50 µL
476 with ultra-pure water. Reactions were mixed by pipetting and briefly centrifuged before
477 incubation at 30˚C for 90 min. Translation of *Firefly* luciferase mRNA (Promega) was quantified
478 using a Victor 2 microplate reader (PerkinElmer).

479

480 Glycosyltransferase activity assay

481 Glycosyltransferase activity was evaluated using GDP- or UDP-Glo™ Glycosyltransferase Assay
482 kits (Promega) with GDP-mannose (VA1095) or UDP-glucose (V6991), respectively, following
483 manufacturers' recommendations. Briefly, 5 µg of purified His_6-SidI and/or molar equivalent (or
484 excess as indicated) SusF were added to 100 µL of 50mM Tris pH 7.4 with 10 µM of GDP-mannose
485 or UDP-glucose. Ten µM GDP or UDP were used as controls as indicated. Reactions were carried
486 out for an hour at 37˚C and quantification of free nucleotide (GDP or UDP) was achieved by
487 addition of GDP- or UDP-Glo™ nucleotide detection reagent following manufacturers'
488 instructions and analyzed via luminescence using a Victor 2 microplate reader (PerkinElmer).

489

490 SDS-PAGE and Western Blot

491 Boiled protein samples were loaded onto either 4-20% gradient SDS-PAGE gels (BioRad), 12% or
492 15% SDS-PAGE gels. Following electrophoresis, proteins were visualized with Coomassie
493 brilliant blue or transferred to PVDF membranes using a BioRad wet transfer cell. Membranes

494 were incubated with blocking buffer [5% nonfat milk powder dissolved in tris-buffered saline-
495 0.1% Tween 20 (TBST)]. Primary antibodies [α-eEF1A (#2551S Cell Signaling Technology), α-Flag-
496 M2 (Sigma), or α-CyaA[3D1] (#EG800 Kerafast)] were used 1:1000 in blocking buffer and detected
497 with HRP-conjugated secondary antibodies (1:5000; ThermoFisher). Membranes were washed,
498 incubated with ECL substrate (GE Amersham) and imaged by chemiluminescence using an
499 Azure Biosystems c300 Darkroom Replacer.

500

501 Surface Plasmon Resonance

502 Direct binding of His_6-SidI to SusF was assessed by SPR using a Biacore T-200 instrument (GE
503 Healthcare) at 25 ˚C, according to the general methods previously described (57). Briefly, all
504 experiments were carried out in a running buffer of HBS-T (20 mM HEPES (pH 7.4), 140 mM
505 NaCl, and 0.005% (v/v) Tween-20 and a flow-rate of 30 µl/min (57). SusF (50 µg mL^{-1} in 10 mM
506 acetate, pH 4.5) was immobilized to a final density of 1063 RU on one flow cell of a CMD-200M
507 surface (XanTec Bioanalytics, GmbH; Dusseldorf, Germany) using standard NHS/EDC coupling.
508 A reference surface was prepared in a similar manner by ethanolamine quenching of NHS/EDC-
509 activated flow cell. Experimental sensorgrams of His_6-SidI binding to immobilized SusF were
510 obtained in reference-corrected, single-cycle mode using sequential concentrations of 0.8, 4, 20,
511 100, and 500 nM His_6-SidI. Each association phase consisted of 2 min sample injection, followed
512 by a 1.5 min dissociation phase, except for the final injection which incorporated a 60 min
513 dissociation phase for more accurate determination of the dissociation rate. Kinetic analysis was

514 performed using Biacore T-200 Evaluation Software v3.1 (GE Healthcare). Sensorgrams were
515 analyzed using both Langmuir and Two-State Reaction binding models and a local value of R_{max}.

516

517 Analytical Gel Filtration Chromatography

518 Samples of recombinant proteins were characterized by analytical-scale gel-filtration
519 chromatography as a mean of assessing their apparent molecular weight. All samples and
520 standards (500 µl total volume) were separated on a Superdex 200 10/300 column (GE Healthcare)
521 attached to an AKTA-format FPLC system using a flow-rate of 0.5 ml/min and PBS as a running
522 buffer. Fractions of 1 ml were collected for subsequent analysis by SDS-PAGE and Coomassie
523 brilliant blue, as described above.

524

525 Molecular Modeling

526 Homology models were created using four different servers, using the full sequence of SidI as
527 inputs and default parameters for each server. Using HHPred (23), a number of templates were
528 identified for residues 376 to 868, and the top 25 templates were forwarded for modeling. Using
529 Phyre2 (24), a smaller region, residues 585 to 763, was chosen for modeling. Raptor-X (20) and I-
530 TASSER (25–27) both produce full-length models. Raptor-X predicted residues 350 to 870 to be a
531 domain. I-TASSER presented five models of low confidence, one of which contained a
532 glycosyltransferase domain with a GT-B fold, which was selected as the working model.

533

534 Statistical Analysis

535 Statistical analysis was performed with GraphPad Prism software using Students' t-test, as
536 indicated, with a 95% confidence interval. For all experiments, data are expressed as mean ±
537 standard deviation (s.d.) of samples in triplicates.

538

539 **Acknowledgements**

540 We thank Drs. Philip Hardwidge and Mary Weber for critical reading of the manuscript and Dr.
541 Craig Roy for providing strains and cell lines. This work was funded through an NIH NIGMS
542 COBRE Research Project Award (P20GM113117; to SRS), a Kansas-INBRE Developmental
543 Research Project Award (P20GM103418; to SRS), a Kansas State University College of Arts and
544 Sciences Undergraduate Research Award (to TJB), a Kansas-INBRE Semester Scholar Award
545 (P20GM103418; to AEP), and start-up funds from Kansas State University (to SRS).

546

547 **References**

548

549 1. Horwitz M. 1983. Formation of a novel phagosome by the Legionnaires' disease bacterium
550 (*Legionella pneumophila*) in human monocytes. The Journal of Experimental Medicine 158:1319
551 1331.
552
553 2. Ensminger AW. 2016. *Legionella pneumophila*, armed to the hilt: justifying the largest arsenal of
554 effectors in the bacterial world. Curr Opin Microbiol 29:74 80.
555
556 3. Ghosh S, O'Connor TJ. 2017. Beyond Paralogs: The Multiple Layers of Redundancy in
557 Bacterial Pathogenesis. Front Cell Infect Microbiol 7:467.
558
559 4. Urbanus ML, Quaile AT, Stogios PJ, Morar M, Rao C, Leo R, Evdokimova E, Lam M, Oatway

C, Cuff ME, Osipiuk J, Michalska K, Nocek BP, Taipale M, Savchenko A, Ensminger AW. 2016. Diverse mechanisms of metaeffector activity in an intracellular bacterial pathogen, *Legionella pneumophila*. Mol Syst Biol 12:893.

5. Kubori T, Shinzawa N, Kanuka H, Nagai H. 2010. *Legionella* metaeffector exploits host proteasome to temporally regulate cognate effector. Plos Pathog 6:e1001216.

6. Shames SR, Liu L, Havey JC, Schofield WB, Goodman AL, Roy CR. 2017. Multiple *Legionella pneumophila* effector virulence phenotypes revealed through high-throughput analysis of targeted mutant libraries. Proc National Acad Sci 63:201708553.

7. Jeong K, Sexton JA, Vogel JP. 2015. Spatiotemporal Regulation of a *Legionella pneumophila* T4SS Substrate by the Metaeffector SidJ. Plos Pathog 11:1 22.

8. Liu Y, Luo Z-Q. 2007. The *Legionella pneumophila* effector SidJ is required for efficient recruitment of endoplasmic reticulum proteins to the bacterial phagosome. Infect Immun 75:592 603.

9. Black MH, Osinski A, Gradowski M, Servage KA, Pawłowski K, Tomchick DR, Tagliabracci VS. 2019. Bacterial pseudokinase catalyzes protein polyglutamylation to inhibit the SidE-family ubiquitin ligases. Science 364:787–792.

10. Bhogaraju S, Bonn F, Mukherjee R, Adams M, Pfleiderer MM, Galej WP, Matkovic V, Lopez-Mosqueda J, Kalayil S, Shin D, Dikic I. 2019. Inhibition of bacterial ubiquitin ligases by SidJ–calmodulin catalysed glutamylation. Nature 572:382–386.

11. Gan N, Zhen X, Liu Y, Xu X, He C, Qiu J, Liu Y, Fujimoto GM, Nakayasu ES, Zhou B, Zhao L, Puvar K, Das C, Ouyang S, Luo Z-Q. 2019. Regulation of phosphoribosyl ubiquitination by a calmodulin-dependent glutamylase. Nature 572:387–391.

12. Shen X, Banga S, Liu Y, Xu L, Gao P, Shamovsky I, Nudler E, Luo Z-Q. 2009. Targeting eEF1A by a *Legionella pneumophila* effector leads to inhibition of protein synthesis and induction of host stress response. Cell Microbiol 11:911 926.

13. Guo Z, Stephenson R, Qiu J, Zheng S, Luo Z-Q. 2014. A *Legionella* effector modulates host cytoskeletal structure by inhibiting actin polymerization. Microbes Infect 16:225–236.

14. Fontana MF, Banga S, Barry KC, Shen X, Tan Y, Luo Z-Q, Vance RE. 2011. Secreted bacterial effectors that inhibit host protein synthesis are critical for induction of the innate immune response to virulent *Legionella pneumophila*. Plos Pathog 7:e1001289.

15. Barry KC, Fontana MF, Portman JL, Dugan AS, Vance RE. 2013. IL-1α signaling initiates the inflammatory response to virulent *Legionella pneumophila in vivo*. J Immunol 190:6329 6339.

16. Moss SM, Taylor IR, Ruggero D, Gestwicki JE, okat K, Mukherjee S. 2019. A *Legionella pneumophila* Kinase Phosphorylates the Hsp70 Chaperone Family to Inhibit Eukaryotic Protein Synthesis. Cell Host Microbe 25:454 462.e6.

17. Belyi Y, Niggeweg R, Opitz B, Vogelsgesang M, Hippenstiel S, Wilm M, Aktories K. 2006. *Legionella pneumophila* glucosyltransferase inhibits host elongation factor 1A. Proc National Acad Sci 103:16953 16958.

18. Belyi Y, Tabakova I, Stahl M, Aktories K. 2008. Lgt: a family of cytotoxic glucosyltransferases produced by *Legionella pneumophila*. J Bacteriol 190:3026 3035.

19. Tzivelekidis T, Jank T, Pohl C, Schlosser A, Rospert S, Knudsen CR, Rodnina MV, Belyi Y, Aktories K. 2011. Aminoacyl-tRNA-charged eukaryotic elongation factor 1A is the bona fide substrate for *Legionella pneumophila* effector glucosyltransferases. Plos One 6:e29525.

20. Källberg M, Wang H, Wang S, Peng J, Wang Z, Lu H, Xu J. 2012. Template-based protein structure modeling using the RaptorX web server. Nat Protoc 7:1511 1522.

21. Nagai H, Cambronne ED, Kagan JC, Amor J, Kahn RA, Roy CR. 2005. A C-terminal translocation signal required for Dot/Icm-dependent delivery of the *Legionella* RalF protein to host cells. P Natl Acad Sci Usa 102:826 831.

22. Huang L, Boyd D, Amyot WM, Hempstead AD, Luo Z-Q, O'Connor TJ, Chen C, Machner M, Montminy T, Isberg RR. 2011. The E Block motif is associated with *Legionella pneumophila* translocated substrates. Cell Microbiol 13:227 245.

23. Söding J, Biegert A, Lupas AN. 2005. The HHpred interactive server for protein homology detection and structure prediction. Nucleic Acids Res 33:W244 8.

24. Kelley LA, Mezulis S, Yates CM, Wass MN, Sternberg MJ. 2015. The Phyre2 web portal for protein modeling, prediction and analysis. Nat Protoc 10:845–858.

25. Yang J, Zhang Y. 2015. I-TASSER server: new development for protein structure and function predictions. Nucleic Acids Res 43:W174–W181.

26. Yang J, Yan R, Roy A, Xu D, Poisson J, Zhang Y. 2015. The I-TASSER Suite: protein structure and function prediction. Nat Methods 12:7–8.

27. Roy A, Kucukural A, Zhang Y. 2010. I-TASSER: a unified platform for automated protein structure and function prediction. Nat Protoc 5:725–738.

28. Holm L. 2019. Benchmarking Fold Detection by DaliLite v.5. Bioinform Oxf Engl. 1-2

29. Kim DE, Chivian D, Malmström L, Baker D. 2005. Automated prediction of domain boundaries in CASP6 targets using Ginzu and RosettaDOM. Proteins Struct Funct Bioinform 61:193–200.

30. Belyi Y, Jank T, Aktories K. 2013. Cytotoxic glucosyltransferases of *Legionella pneumophila*. Curr Top Microbiol 376:211 226.

31. Price CT, Al-Quadan T, Santic M, Rosenshine I, Kwaik Y. 2011. Host proteasomal degradation generates amino acids essential for intracellular bacterial growth. Science 334:1553 1557.

32. Belyi Y, Tartakovskaya D, Tais A, Fitzke E, Tzivelekidis T, Jank T, Rospert S, Aktories K. 2012. Elongation factor 1A is the target of growth inhibition in yeast caused by *Legionella pneumophila* glucosyltransferase Lgt1. J Biol Chem 287:26029 26037.

33. Dever TE, Green R. 2012. The Elongation, Termination, and Recycling Phases of Translation in Eukaryotes. Csh Perspect Biol 4:a013706.

34. Belyi Y, Stahl M, Sovkova I, Kaden P, Luy B, Aktories K. 2009. Region of elongation factor 1A1 involved in substrate recognition by *Legionella pneumophila* glucosyltransferase Lgt1: identification of Lgt1 as a retaining glucosyltransferase. J Biol Chem 284:20167 20174.

35. Rolando M, Buchrieser C. 2014. *Legionella pneumophila* type IV effectors hijack the transcription and translation machinery of the host cell. Trends Cell Biol 24:771 778.

36. Shamovsky I, Ivannikov M, Kandel ES, Gershon D, Nudler E. 2006. RNA-mediated response to heat shock in mammalian cells. Nature 440:556–560.

37. Vera M, Pani B, Griffiths LA, Muchardt C, Abbott CM, Singer RH, Nudler E. 2014. The translation elongation factor eEF1A1 couples transcription to translation during heat shock response. Elife 3:e03164.

38. Yan L, Cerny RL, Cirillo JD. 2004. Evidence that hsp90 is involved in the altered interactions of *Acanthamoeba castellanii* variants with bacteria. Eukaryot Cell 3:567 578.

39. Havey JC, Roy CR. 2015. Toxicity and SidJ-Mediated Suppression of Toxicity Require Distinct Regions in the SidE Family of *Legionella pneumophila* Effectors. Infect Immun 83:3506 3514.

40. Wang Y, Shi M, Feng H, Zhu Y, Liu S, Gao A, Gao P. 2018. Structural Insights into Non-canonical Ubiquitination Catalyzed by SidE. Cell 173:1231-1243.e16.

689 41. Dong Y, Mu Y, Xie Y, Zhang Y, Han Y, Zhou Y, Wang W, Liu Z, Wu M, Wang H, Pan M, Xu
690 N, Xu C-Q, Yang M, Fan S, Deng H, Tan T, Liu X, Liu L, Li J, Wang J, Fang X, Feng Y. 2018.
691 Structural basis of ubiquitin modification by the *Legionella* effector SdeA. Nature 557:674–678.
692
693 42. Qiu J, Sheedlo MJ, Yu K, Tan Y, Nakayasu ES, Das C, Liu X, Luo Z-Q. 2016. Ubiquitination
694 independent of E1 and E2 enzymes by bacterial effectors. Nature 533:120 124.
695
696 43. Sethi MK, Buettner FF, Ashikov A, Bakker H. 2013. Glycosyltransferases, Methods and
697 Protocols 307–320.
698
699 44. Mishra AK, Krumbach K, Rittmann D, Batt SM, Lee O, De S, Frunzke J, Besra GS, Eggeling
700 L. 2012. Deletion of manC in *Corynebacterium glutamicum* results in a phospho-myo-inositol
701 mannoside- and lipoglycan-deficient mutant. Microbiology+ 158:1908–1917.
702
703 45. Rodrigo-Unzueta A, Martínez MA, Comino N, Alzari PM, Chenal A, Guerin ME. 2016.
704 Molecular Basis of Membrane Association by the Phosphatidylinositol Mannosyltransferase
705 PimA Enzyme from Mycobacteria. J Biol Chem 291:13955–13963.
706
707 46. Panda S, Saxena S, Guruprasad L. 2019. Homology modeling, docking and structure-based
708 virtual screening for new inhibitor identification of *Klebsiella pneumoniae* heptosyltransferase-III.
709 J Biomol Struct Dyn 1–16.
710
711 47. Batt SM, Jabeen T, Mishra AK, Veerapen N, Krumbach K, Eggeling L, Besra GS, Fütterer K.
712 2010. Acceptor Substrate Discrimination in Phosphatidyl-myo-inositol Mannoside Synthesis
713 STRUCTURAL AND MUTATIONAL ANALYSIS OF MANNOSYLTRANSFERASE
714 CORYNEBACTERIUM GLUTAMICUM PimB′. J Biol Chem 285:37741–37752.
715
716 48. Coates S, Gurney T, Sommers L, Yeh M, Hirschberg C. 1980. Subcellular localization of sugar
717 nucleotide synthetases. J Biol Chem 255:9225–9.
718
719 49. Kawakita M, Ishida N, Miura N, Sun-Wada G, Yoshioka S. 1998. Nucleotide sugar
720 transporters: elucidation of their molecular identity and its implication for future studies. J
721 Biochem 123:777–85.
722
723 50. Berger K, Isberg R. 1993. Two distinct defects in intracellular growth complemented by a
724 single genetic locus in *Legionella pneumophila*. Mol Microbiol 7:7 19.
725
726 51. Roy CR, Berger KH, Isberg RR. 1998. *Legionella pneumophila* DotA protein is required for
727 early phagosome trafficking decisions that occur within minutes of bacterial uptake. Mol
728 Microbiol 28:663–674.
729
730 52. Feeley J, Gibson R, Gorman G, Langford N, Rasheed J, Mackel D, Baine W. 1979. Charcoal-
731 yeast extract agar: primary isolation medium for *Legionella pneumophila*. J Clin Microbiol 10:437

441.

53. Saito A, Rolfe R, Edelstein P, Finegold S. 1981. Comparison of liquid growth media for *Legionella pneumophila*. J Clin Microbiol 14:623 627.

54. Joiner K, Fuhrman S, Miettinen H, Kasper L, Mellman I. 1990. *Toxoplasma gondii*: fusion competence of parasitophorous vacuoles in Fc receptor-transfected fibroblasts. Science 249:641–646.

55. Geisbrecht BV, Bouyain S, Pop M. 2006. An optimized system for expression and purification of secreted bacterial proteins. Protein Expres Purif 46:23–32.

56. Ingmundson A, Delprato A, Lambright DG, Roy CR. 2007. *Legionella pneumophila* proteins that regulate Rab1 membrane cycling. Nature 450:365–369.

57. Stapels D, Woehl JL, Milder FJ, Tromp AT, van Batenburg AA, de Graaf WC, Broll SC, White NM, Rooijakkers S, Geisbrecht BV. 2018. Evidence for multiple modes of neutrophil serine protease recognition by the EAP family of Staphylococcal innate immune evasion proteins. Protein Sci 27:509–522.

Tables

Table 1. Oligonucleotide primers used in this study

Name	Sequence (5′ → 3′) [a]
SusFSalI-F	att**gtcgaca**atgataaaaggaaaacttatgccc
SusFBglII-F	tgg**agatct**atgataaaaggaaaacttatgc
SusFPstI-R	gg**ctgcag**ttataaaataattggtcgag
SidIBamHI-F2	att**ggatcc**ttatgactaaaatatacttattaactgc
SidIBamHI-F	att**ggatcc**atgactaaaatatacttattaactgc
SidINotI-R	att**gcggccgc**tcaaaataccagtatcgattctttaag
SidICBamHI-F	att**ggatcc**atgaatttttatgattttgatgg
SidICΔ68NotI-R	att**gcggccgc**tcatatattctctaataaatgatc

SidINNotI-R	att**gcggccgc**tcatctgaaacttttatcgtgctc
SidIPstI-R	att**ctgcag**tcaaaataccagtatcgattc

[a]-restriction endonuclease cleavage sites are shown in bold

Figure Legends

Figure 1. SusF and SidI interact directly with nanomolar affinity. (A) Lysates from HEK 293 cells stably expressing 3FLAG-SusF were incubated with glutathione beads coated with either GST or GST-SidI followed by Coomassie staining for total protein and Western blotting for SusF (α-FLAG). Arrowheads indicate GST and GST-SidI proteins. **(B)** Lysates from *E. coli* overexpressing either GST or GST-SidI were incubated with Ni-NTA beads coated with His_6-SusF followed by SDS-PAGE and Coomassie staining for proteins retained on the beads. Left panel: whole cell lysates from uninduced and induced cultures of *E. coli* expressing GST and GST-SidI proteins; Right panel: proteins retained on Ni-NTA beads (see *Materials and Methods*). **(C)** Chromatograms resulting from analytical scale gel-filtration separation of either SusF alone (green trace) or SusF bound to SidI (red trace). A chromatogram of known size standards is provided for reference (blue trace). **(D)** Binding of His_6-SidI to immobilized SusF was assessed by SPR. The reference corrected sensorgram from a single-cycle experiment is shown in black, while the outcome of fitting to a two-state binding model is shown in red. The interaction is described by an apparent K_D of 3.1 nM, consisting of two individual steps where $k_{on,1} = 2.7x10^4\ M^{-1}s^{-1}$ and $k_{off,1} = 5.1x10\text{-}4\ s^{-1}$ and $k_{on,2} = 2.3x10^{-3}\ s^{-1}$ and $k_{off,2} = 4.5x10^{-4}\ s^{-1}$, respectively.

773 **Figure 2. SusF modulates SidI-mediated translation inhibition *in vitro*.** Translation of luciferase
774 mRNA was quantified using a rabbit reticulocyte lysate kit. Translation of luciferase in the
775 presence of **(A)** 4 ng His_6-SidI or 20 ng SusF; **(B)** His_6-SidI alone or 4 ng (37 fmol) His_6-SidI and an
776 equimolar amount of SusF (37 fmol); **(C)** His_6-SidI alone or His_6-SidI and SusF were added to *in*
777 *vitro* translation reactions at the indicated times (-30 indicates pre-incubation of His_6-SidI and
778 SusF for 30 min prior to translation reaction); **(D)** Quantification of *In vitro* translation of Luc
779 mRNA in the presence of His_6-SidI alone or His_6-SidI and SusF at increasing molar ratios (1:1, 2:1
780 and 5:1 molar ratios of SusF:His_6-SidI). Data are representative of at least two independent
781 experiments and shown as mean ± s.d. of samples in triplicates. Asterisks denote statistical
782 significance by *t*-test (*P<0.05, **P<0.01; n.s., not significant).

783

784 **Figure 3. SusF does not impair interaction between SidI and eEF1A. (A)** GST-SusF or GST alone
785 were immobilized on magnetic glutathione agarose beads followed by incubation with 100 μg
786 purified His_6-SidI alone or that had been preincubated with lysates from HEK 293T cells as
787 indicated (Lysates). Proteins were separated by SDS-PAGE and visualized by Coomassie staining
788 or Western blot as indicated. **(B)** Lysates from *E. coli* expressing GST-SidI or GST alone were
789 incubated with magnetic glutathione agarose beads and lysates from HEK 293T followed by 10,
790 to 1000 μg of purified recombinant SusF (shown as increasing amounts in supernatants from
791 beads). Proteins remaining on the beads were separated by SDS-PAGE and visualized by
792 Coomassie stain or Western blot as indicated. GST-SidI (~130 kDa) and SusF (~27 kDa) are
793 indicated with arrowheads. Data are representative of at least two independent experiments.

Figure 4. SusF and eEF1A interact with distinct regions of SidI. (A) Schematic representation of SidI truncation proteins. **(B)** Lysates from *E. coli* expressing GST-SidI constructs were incubated with glutathione agarose beads followed by washing and incubation with lysates from HEK 293 cells stably expressing 3FLAG-SusF as indicated. Proteins were separated by SDS-PAGE and visualized by Coomassie stain (GST-SidI) or Western blot. Arrowheads indicate fusion proteins. Data are representative of three independent experiments.

Figure 5. SusF is not required for Dot/Icm translocation of SidI into host cells. (A) Western blot showing production of CyaA-RalF (~76 kDa) and CyaA-SidI$_{RP}$ (~150 kDa) by the indicated *L. pneumophila* strains. **(B)** Quantification of cAMP extracted from CHO FcγRII cells infected with the indicated *L. pneumophila* strains. Asterisks denote statistical significance by *t*-test (**P<0.01). Data are representative of two independent experiments (n.s., not significant).

Figure 6. Full-length SidI is required for translation inhibition. Translation of luciferase mRNA quantified using a rabbit reticulocyte lysate kit. **(A)** Translation of luciferase mRNA in the presence of **(A)** 4 ng His$_6$-SidI, His$_6$-SidI$_N$, His$_6$-SidI$_C$, or His$_6$-SidI$_{CΔ68}$ or (**B)** 4 ng of His$_6$-SidI alone or increasing amounts of His$_6$-SidI$_{CΔ68}$ (4 ng, 50 ng, 100 ng). Asterisks denote statistical significance by *t*-test (**P<0.01). Data are representative of at least two independent experiments.

814 **Figure 7. SidI possesses glycosyltransferase activity. (A)** Quantification of GDP liberated from
815 GDP-mannose in the presence or absence of 5 μg purified His_6-SidI. **(B)** Quantification of UDP
816 liberated from UDP-glucose in the presence or absence of 5 μg purified His_6-SidI. Quantification
817 of free GDP from GDP-mannose in the presence or absence of **(C)** 5 μg His_6-SidI full-length or
818 truncated proteins, **(D)** 5 μg His_6-SidI and/or molar equivalent of SusF, or **(E)** increasing molar
819 amount of SusF (1:1, 2:1, or 5:1 molar ratio of SusF:His_6-SidI). Asterisks denote statistical
820 significance by *t*-test (**P<0.01 and *P<0.05). Data are representative of at least two independent
821 experiments.

822

823 **Supplemental Information**

824 **Supplemental Figure Legends**

825 **Figure S1. Co-elution of SusF and SidI by gel filtration chromatography.** A sample of
826 recombinant SidI bound to SusF was separated by analytical scale gel filtration chromatography
827 as presented in Figure 1C. Ten μl of each column fraction were analyzed by SDS-PAGE followed
828 by Coomassie staining to assess the protein content within each fraction. Fractions corresponding
829 to the peak of approximately 150 kDa apparent molecular weight in the sample of SidI bound to
830 SusT (Fig. 1C, red trace) contained both proteins, consistent with formation of a 1:1 complex
831 between these two molecules.

832

833 **Figure S2. Binding of His_6-SidI to immobilized SusF was assessed by SPR**. The reference
834 corrected sensorgram from a single-cycle experiment is shown in black, while the outcome of
835 fitting to a Langmuir binding model is shown in red. Using this model, the interaction is
836 described by an apparent K_D of 0.89 nM where k_{on} = $2.2x10^5$ $M^{-1}s^{-1}$ and k_{off} = $1.9x10^{-4}$ s^{-1} ,
837 respectively.

838

839 **Figure S3. eEF1A interacts with the SidI-SusF complex.** Lysates from *E. coli* expressing GST-SidI
840 or GST alone were incubated with magnetic glutathione agarose beads and washed followed by
841 addition of 10, 25, 50, 100, 200, 400, 800 or 1000 μg of purified recombinant SusF (shown as
842 increasing amounts in supernatants from beads). Beads were subsequently incubated with lysates
843 from HEK 293T cells. Proteins remaining on the beads were separated by SDS-PAGE and
844 visualized by Coomassie stain or Western blot

845

846 **Figure S4. Molecular model of SidI.** Ribbon cartoons of SidI modeled using the RaptorX
847 webserver. Putative SidI domains are shown in red (residues 1-268), magenta (residues 269-874)
848 and cyan (residues 874-942).

849

850 **Figure S5. Interaction between eEF1A and SidI truncations in the absence of SusF.** Lysates from
851 *E. coli* expressing GST-SidI constructs were incubated with glutathione agarose beads followed
852 by washing and incubation with lysates from HEK 293 cells. Proteins were separated by SDS-

853 PAGE and visualized by Coomassie staining (GST-SidI) or Western blotting (eEF1A). Data are
854 representative of two independent experiments.

855

856 **Figure S6. SidI is modeled as a glycosyltransferase with a GT-B fold.** The model of the putative
857 glycosyltransferase domain is presented in magenta ribbons superimposed to that of PimB (PDB:
858 3OKA) represented as salmon ribbons, which was identified by DALI as the most similar
859 structure in the PDB. The structure of PimB was solved in the presence of GDP (salmon spheres).

860

Figure 1

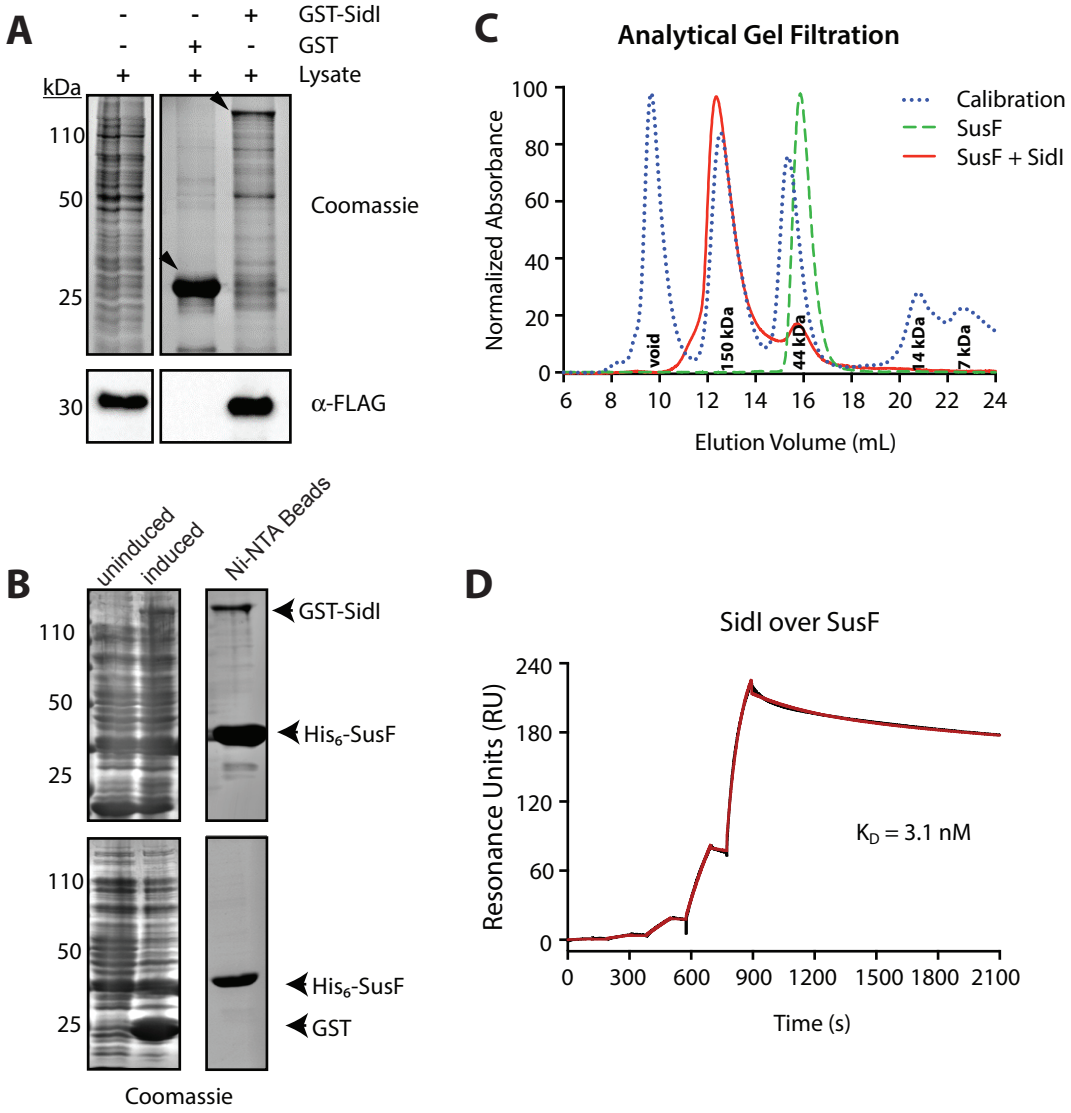

Figure 2

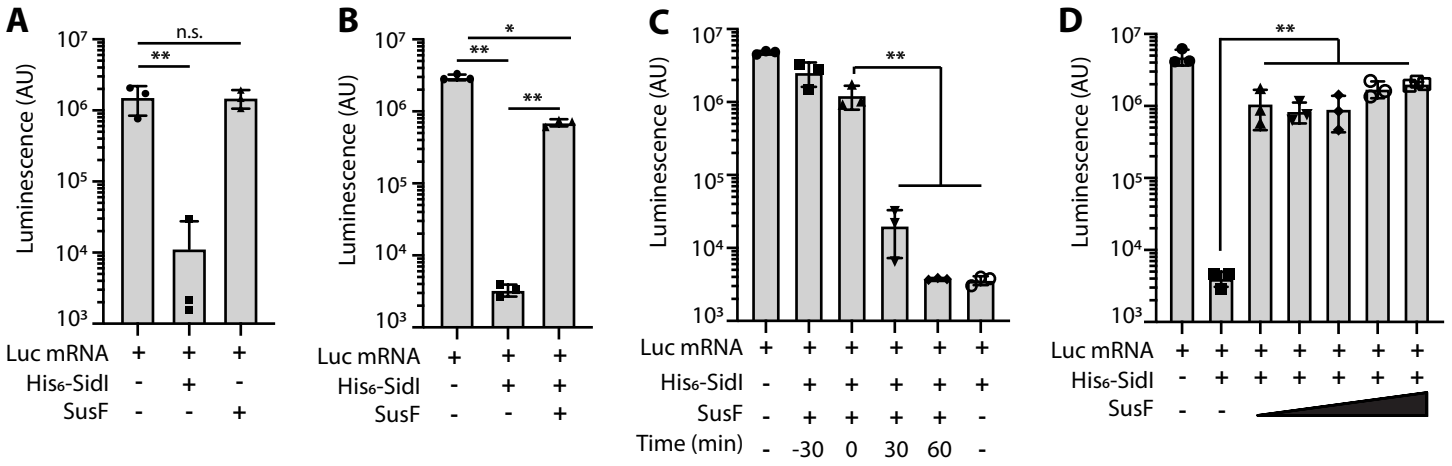
A
B
C
D
Luminescence (AU)
n.s.
*
**
Luc mRNA
His6-SidI
SusF
Time (min)
-30
0
30
60

Figure 3

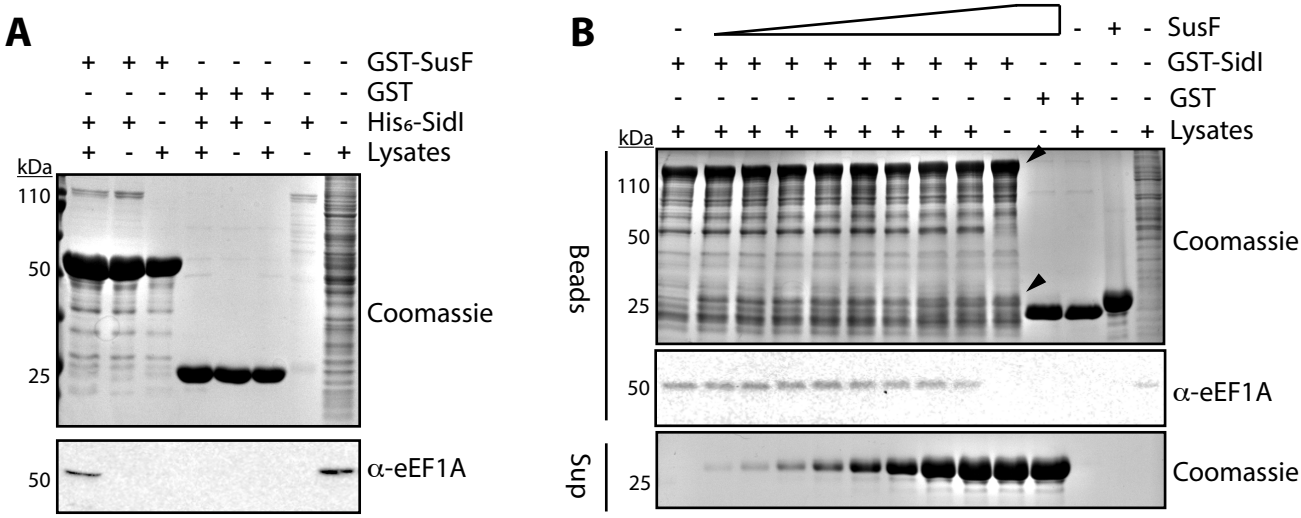

Figure 4

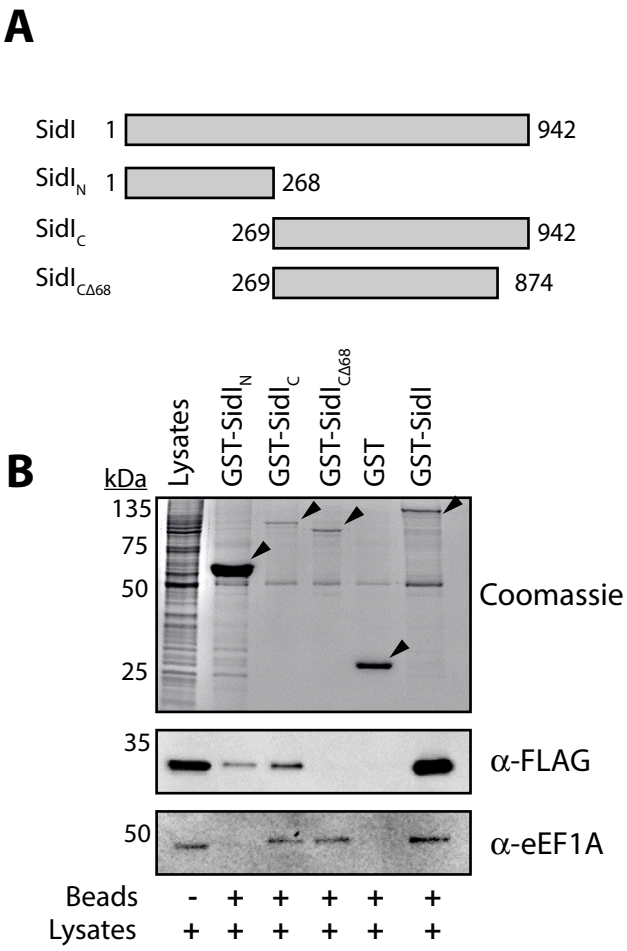

Figure 5

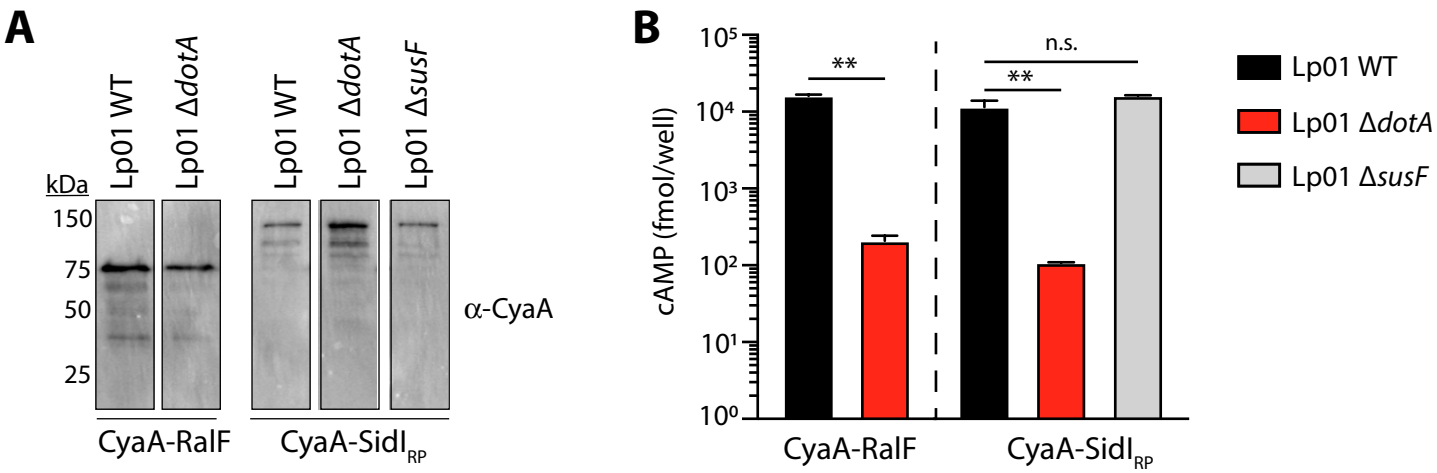

Figure 6

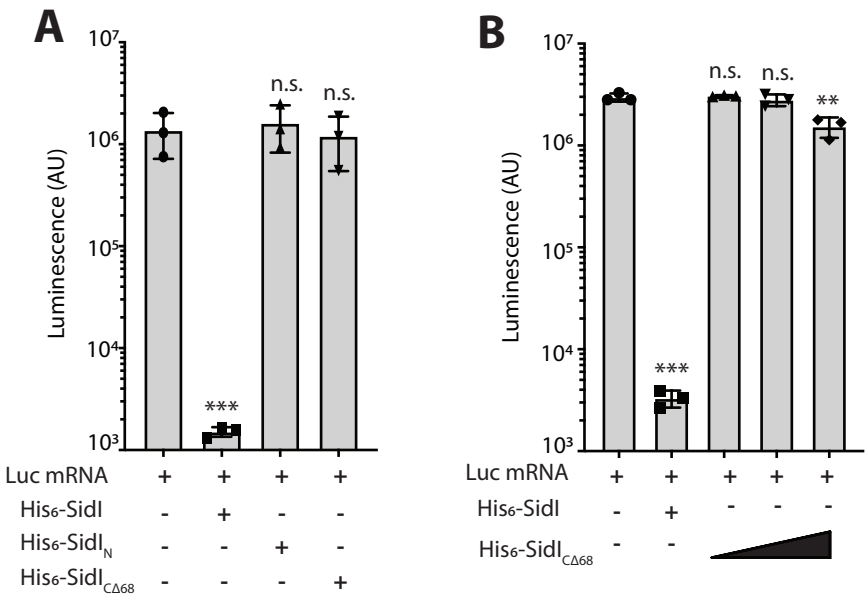

Figure 7

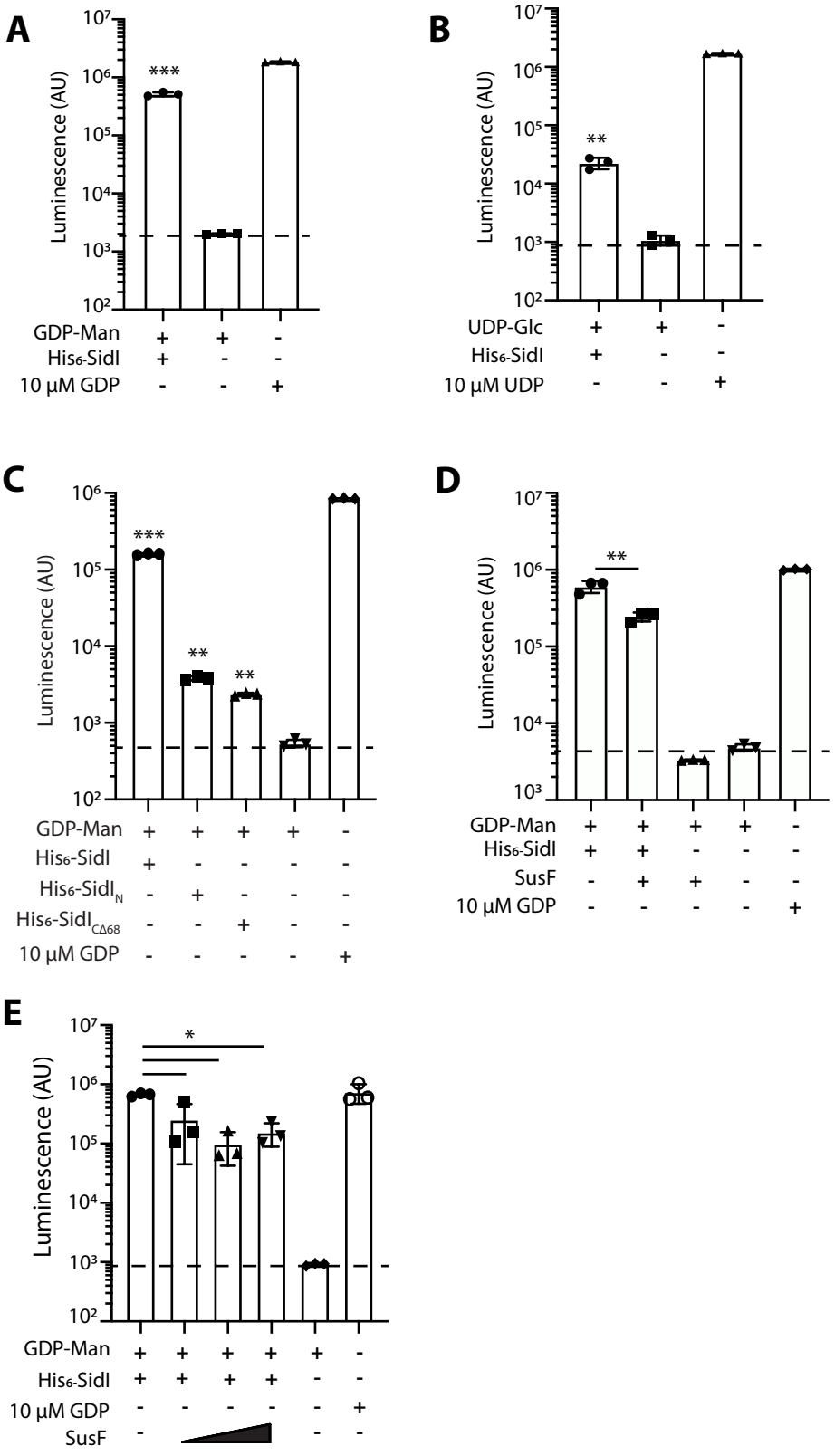

Figure S1

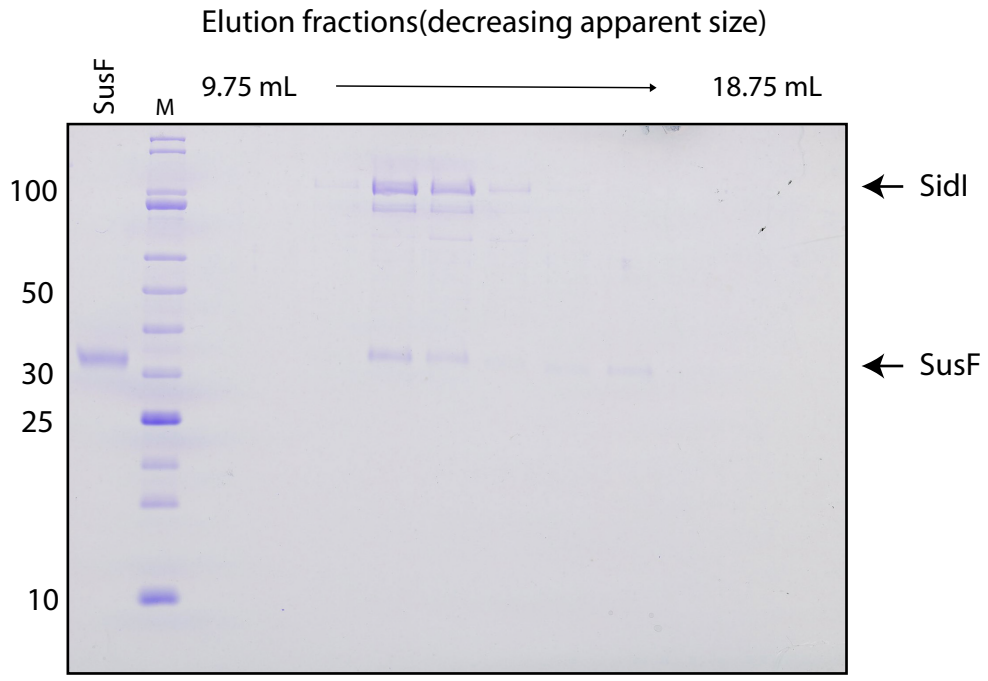

Figure S2

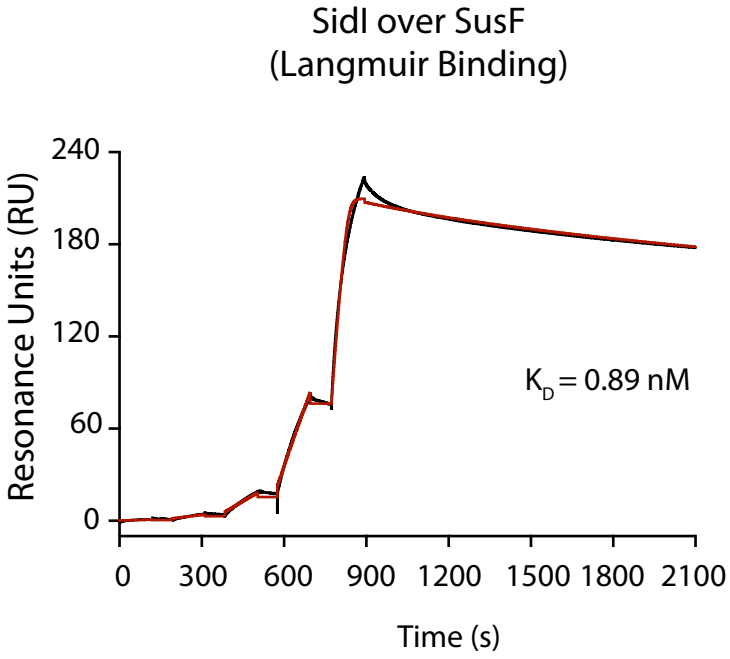

Figure S3

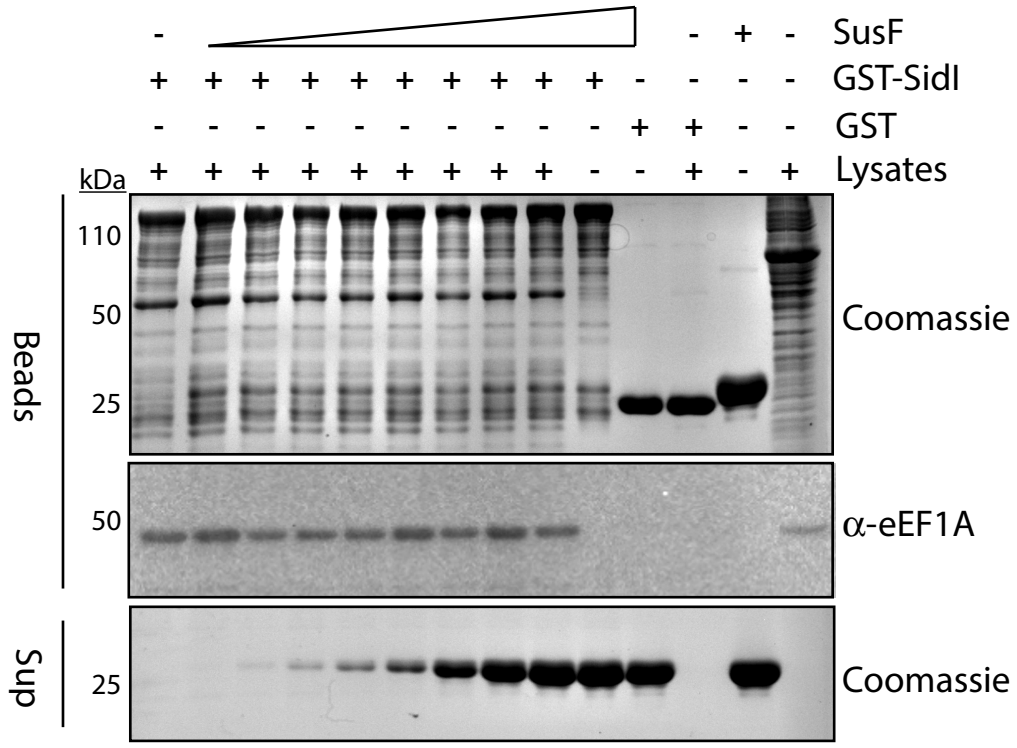

Figure S4

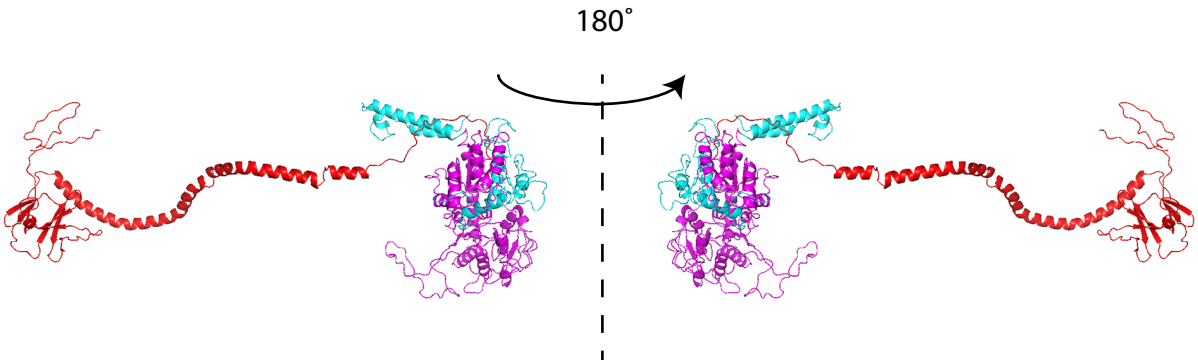

Figure S5

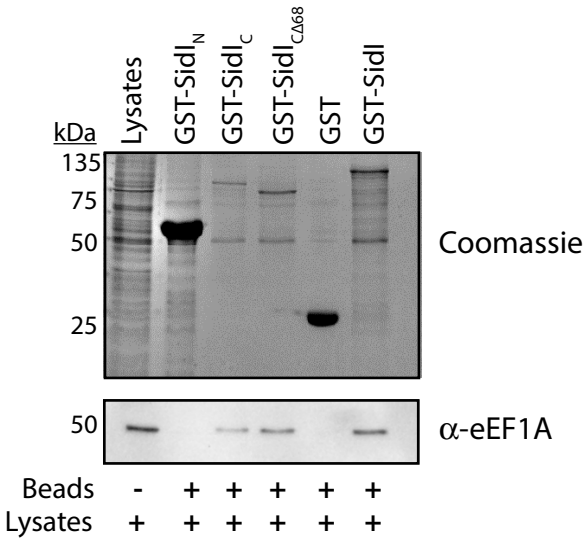

Figure S6

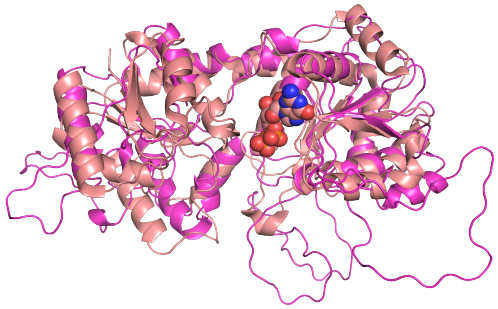

Supplemental Tables

Table S1. Proteins with homology to SidI (HHPred).

No.	PDB		Prob	E-value	P-value	Score	SS	Cols	Query HMM	Template HMM
1	3OKP_A	GDP-mannose-dependent a	99.8	8.2E-20	1.7E-24	181.2	33.6	338	376-868	22-376 (394)
2	4N9W_A	GDP-mannose-dependent a	99.8	3.7E-19	7.5E-24	175.7	36.7	342	370-868	17-364 (390)
3	5D01_B	N-acetyl-alpha-D-glucos	99.8	2.3E-19	4.7E-24	175.8	34.1	347	370-868	15-372 (379)
4	6D9T_A	Glycosyl transferase (E	99.8	1.3E-18	2.6E-23	173.7	33.4	348	370-868	30-387 (400)
5	2JJM_J	GLYCOSYL TRANSFERASE, G	99.8	1.1E-18	2.3E-23	174.8	32.9	346	372-868	27-382 (394)
6	3C48_A	Predicted glycosyltrans	99.8	3.6E-18	7.2E-23	172.6	35.2	352	370-868	40-422 (438)
7	3FRO_B	GlgA glycogen synthase	99.8	5.5E-18	1.1E-22	169.0	34.6	347	370-868	16-427 (439)
8	2R60_A	Glycosyl transferase, g	99.8	1.1E-17	2.3E-22	172.5	37.8	351	370-868	31-456 (499)
9	3OY2_B	Glycosyltransferase B73	99.7	1.3E-18	2.6E-23	176.1	28.3	339	376-868	17-387 (413)
10	6EJI_B	WlaC protein; Glycosylt	99.7	2E-17	4.1E-22	162.9	33.8	333	373-868	15-354 (373)
11	6GNE_A	Probable starch synthas	99.7	8.5E-18	1.7E-22	176.0	31.4	352	369-868	23-494 (508)
12	2QZS_A	PROTEIN; glycosyl-trans	99.7	1.6E-17	3.2E-22	171.3	28.9	347	371-869	16-474 (485)
13	2X6Q_A	TREHALOSE-SYNTHASE TRET	99.7	7.6E-17	1.5E-21	161.9	31.8	386	328-868	8-411 (416)
14	4XYW_A	O-antigen biosynthesis	99.7	1.4E-16	2.8E-21	155.5	31.5	315	376-868	17-336 (338)
15	4XSO_A	Glycosyltransferase (E.	99.7	4.4E-17	8.9E-22	162.6	28.5	291	429-868	81-381 (388)
16	1RZV_A	Glycogen synthase 1 (E.	99.7	2.3E-16	4.6E-21	162.3	33.7	344	371-868	16-472 (485)
17	1V4V_B	UDP-N-Acetylglucosamine	99.7	5.1E-17	1E-21	160.9	25.2	341	370-869	13-366 (376)
18	2IW1_A	LIPOPOLYSACCHARIDE CORE	99.7	4.5E-16	9.2E-21	150.8	31.0	344	372-868	14-368 (374)
19	5ENZ_A	UDP-GlcNAc 2-epimerase	99.6	1.3E-16	2.6E-21	159.1	26.6	344	367-869	6-366 (385)
20	1XV5_A	DNA alpha-glucosyltrans	99.6	8.9E-17	1.8E-21	163.7	25.6	348	370-868	13-399 (401)
21	2X0D_B	WSAF; GT4 FAMILY, TRANS	99.6	9E-16	1.8E-20	155.5	31.7	335	369-868	60-413 (413)
22	5N7Z_A	Lipopolysaccharide 1,6-	99.6	1.5E-15	3.1E-20	147.4	31.5	339	372-868	14-357 (359)
23	5E9T_C	Glycosyltransferase Gtf	99.6	1E-15	2E-20	163.6	32.1	312	388-868	169-497 (503)
24	1VGV_D	UDP-N-acetylglucosamine	99.6	1.9E-16	3.8E-21	156.8	24.3	340	367-868	5-369 (384)
25	3T7D_A	Putative glycosyltransf	99.6	5.8E-16	1.2E-20	169.6	30.2	297	430-868	136-471 (497)
26	4FKZ_B	UDP-N-acetylglucosamine	99.6	2.8E-16	5.7E-21	157.8	24.4	334	377-869	18-368 (388)
27	5DLD_A	UDP-N-Acetylglucosamine	99.6	4.3E-16	8.6E-21	158.4	25.6	338	369-868	16-378 (413)
28	3VUE_A	Granule-bound starch sy	99.6	3.1E-15	6.2E-20	162.0	32.3	350	372-868	26-508 (536)
29	5UOF_B	Alpha,alpha-trehalose-p	99.6	3.9E-16	7.9E-21	167.1	24.3	281	443-868	131-461 (481)

30	3DZC_B	UDP-N-acetylglucosamine	99.6	5.8E-16	1.2E-20	156.0	23.7	331	378-866	41-396	(396)
31	6GNF_A	Glycogen synthase (E.C.	99.6	5.4E-15	1.1E-19	160.0	31.7	345	369-868	35-536	(544)
32	3S28_H	Sucrose synthase 1 (E.C	99.6	3.6E-15	7.3E-20	176.5	32.3	341	382-868	320-766	(816)
33	6GNG_A	Granule-bound starch sy	99.6	5.7E-15	1.2E-19	165.6	32.2	347	368-868	52-556	(612)
34	3OT5_B	UDP-N-acetylglucosamine	99.6	1.1E-15	2.2E-20	154.9	23.3	333	378-869	43-393	(403)
35	4HWG_A	UDP-N-acetylglucosamine	99.6	7.2E-16	1.5E-20	155.2	21.7	342	369-869	16-375	(385)
36	4X7R_B	TarM; Glycosyltransfera	99.6	7.7E-15	1.6E-19	162.3	31.8	283	429-869	204-492	(493)
37	5LQD_D	Alpha,alpha-trehalose-p	99.6	4.7E-15	9.6E-20	159.7	29.0	287	443-868	146-462	(465)
38	4HLN_A	Starch synthase I (E.C.	99.6	1.1E-14	2.2E-19	163.4	33.0	343	369-868	138-622	(633)
39	4PQG_A	Glycosyltransferase Gtf	99.6	4.5E-15	9.1E-20	160.2	28.8	285	427-868	203-505	(511)
40	5JIO_A	Alpha,alpha-trehalose-p	99.5	5.3E-15	1.1E-19	156.1	25.3	307	443-868	136-474	(487)
41	4L22_A	Phosphorylase (E.C.2.4.	99.5	2.8E-15	5.8E-20	176.9	25.4	298	442-868	269-754	(758)
42	5HVO_C	trehalose-6-phosphate p	99.5	4.5E-15	9E-20	160.5	24.7	285	443-868	141-474	(479)
43	3S2U_A	UDP-N-acetylglucosamine	99.5	3.4E-14	7E-19	138.8	27.3	316	372-868	13-355	(365)
44	4W6Q_A	Glcosyltransferase C; G	99.5	4.2E-14	8.4E-19	139.3	27.5	276	417-868	38-330	(333)
45	4NES_A	UDP-N-acetylglucosamine	99.5	3.5E-15	7.2E-20	147.7	20.0	332	367-868	5-361	(374)
46	4RBN_B	Sucrose synthase:Glycos	99.5	7.8E-14	1.6E-18	165.4	31.1	299	430-868	378-754	(794)
47	4AMG_A	SNOGD; TRANSFERASE, POL	99.5	3.9E-14	7.9E-19	140.7	23.7	322	372-869	33-400	(400)
48	3RHZ_B	Nucleotide sugar synthe	99.5	9.8E-14	2E-18	136.6	26.1	279	414-868	44-334	(339)
49	3IA7_A	CalG4; Glycosysltransfe	99.5	3.1E-14	6.3E-19	139.0	22.3	343	372-869	15-398	(402)
50	5W8X_A	Lipid-A-disaccharide sy	99.5	8.6E-14	1.7E-18	137.4	25.3	324	370-868	15-377	(382)
51	2P6P_B	Glycosyl transferase; C	99.4	2.5E-13	5E-18	134.3	27.3	319	372-868	11-378	(384)
52	2IUY_A	GLYCOSYLTRANSFERASE; GL	99.4	1.5E-13	3.1E-18	136.3	25.7	296	370-868	28-332	(342)
53	5VAF_B	Accessory Sec system pr	99.4	6.3E-14	1.3E-18	152.9	24.9	282	429-869	214-520	(533)
54	5V0T_B	Alpha,alpha-trehalose-p	99.4	7.6E-14	1.5E-18	152.3	25.2	303	429-868	116-465	(494)
55	1UQT_B	ALPHA, ALPHA-TREHALOSE-	99.4	1.1E-13	2.3E-18	150.2	26.2	300	430-868	111-451	(482)
56	4RIF_B	Glycosyl transferase ho	99.4	3.8E-14	7.8E-19	140.7	20.1	321	370-868	9-373	(379)
57	5DXF_A	trehalose-6-phosphate p	99.4	2.9E-13	5.8E-18	150.5	29.1	313	430-868	185-523	(534)
58	1F0K_A	E. COLI MURG (E.C. 2.4.	99.4	1.8E-12	3.6E-17	127.8	30.3	311	370-868	15-354	(364)
59	3TSA_A	NDP-rhamnosyltransferas	99.4	2.1E-13	4.3E-18	134.2	23.5	320	372-868	12-387	(391)
60	5HVL_B	trehalose-6-phosphate p	99.4	2.4E-13	4.8E-18	146.1	25.8	286	443-868	134-467	(478)
61	6INF_A	UDP-glycosyltransferase	99.4	5.4E-13	1.1E-17	133.6	26.2	332	373-867	24-454	(466)
62	3RSC_B	CalG2; TDP, enediyne, S	99.4	6.8E-13	1.4E-17	131.3	26.5	320	372-868	31-412	(415)
63	3NB0_C	Glycogen [starch] synth	99.4	1.8E-13	3.6E-18	158.6	25.4	287	429-868	164-630	(725)
64	5I45_A	Glycosyl transferases g	99.4	2.2E-13	4.4E-18	126.1	20.9	181	585-868	27-209	(218)
65	5ZFK_A	UDP-glucose:tetrahydrob	99.4	9.6E-13	1.9E-17	127.7	26.2	325	372-868	21-348	(354)

932	66	2HY7_A	Crystal Structure of Gu	99.4	3.9E-13	8E-18	137.4	24.7	258	429-867	103-373 (406)
933	67	2XCI_C	3-DEOXY-D-MANNO-2-OCTUL	99.4	5.3E-13	1.1E-17	138.5	25.6	312	376-868	53-374 (374)
934	68	5ZLR_A	NeuC protein; NeuC, UDP	99.4	5.2E-13	1.1E-17	132.2	24.0	315	376-868	18-364 (380)
935	69	3OTI_B	CalG3; Calicheamicin, T	99.3	6.1E-13	1.2E-17	131.7	21.7	323	370-868	29-396 (398)
936	70	5DU2_A	CalS8; glycosyltransfer	99.3	1.1E-12	2.3E-17	129.9	23.1	322	372-868	37-415 (419)
937	71	1L5W_A	MALTODEXTRIN PHOSPHORYL	99.3	2.1E-13	4.2E-18	162.7	21.2	346	429-868	277-791 (796)
938	72	4FZR_A	SsfS6; Structural Genom	99.3	4.4E-13	8.9E-18	132.7	19.6	319	372-866	26-397 (398)
939	73	3OTG_A	CalG1; Calicheamicin, T	99.3	3.3E-12	6.6E-17	129.3	24.4	324	370-868	29-407 (412)
940	74	4QLB_D	Probable glycogen [star	99.3	2.6E-12	5.4E-17	150.1	26.4	297	429-868	178-632 (674)
941	75	3HBJ_A	Flavonoid 3-O-glucosylt	99.3	1.8E-11	3.6E-16	124.1	28.6	328	378-868	30-452 (454)
942	76	2IYA_B	OLEANDOMYCIN GLYCOSYLTR	99.2	7.4E-12	1.5E-16	122.5	23.6	322	371-868	22-420 (424)
943	77	4X1T_A	Monogalactosyldiacylgly	99.2	3.8E-11	7.7E-16	120.7	27.5	324	372-868	17-384 (408)
944	78	2ACV_B	triterpene UDP-glucosyl	99.2	3.7E-11	7.5E-16	122.1	27.2	337	372-868	20-461 (463)
945	79	2YJN_A	GLYCOSYLTRANSFERASE, DT	99.2	2.5E-12	5.1E-17	129.2	18.4	323	372-869	31-435 (441)
946	80	2VSY_B	XCC0866; TRANSFERASE, G	99.2	1.9E-11	3.9E-16	135.3	26.9	326	371-868	217-556 (568)
947	81	3QHP_A	Type 1 capsular polysac	99.2	6.1E-12	1.2E-16	110.8	17.6	163	586-863	1-166 (166)
948	82	3WAD_B	Glycosyltransferase; GL	99.2	1.6E-11	3.2E-16	121.0	20.8	316	371-868	10-413 (419)
949	83	4ZHT_B	Bifunctional UDP-N-acet	99.2	2.4E-11	4.9E-16	124.2	22.7	268	429-868	92-374 (411)
950	84	2C4M_A	GLYCOGEN PHOSPHORYLASE	99.1	2.4E-11	4.9E-16	145.7	25.8	301	442-868	287-785 (796)
951	85	5DJS_B	Tetratricopeptide TPR_2	99.1	1.1E-10	2.2E-15	128.0	26.9	330	370-868	173-512 (529)
952	86	2GJ4_A	Glycogen phosphorylase,	99.1	2.6E-10	5.3E-15	137.7	30.3	295	442-868	318-813 (824)
953	87	5GL5_B	Sterol 3-beta-glucosylt	99.1	2.6E-10	5.3E-15	117.1	25.5	358	373-868	51-459 (498)
954	88	5E9T_D	Glycosyltransferase Gtf	99.0	6.5E-11	1.3E-15	129.3	21.3	230	475-869	215-446 (447)
955	89	2BFW_A	GLGA GLYCOGEN SYNTHASE	99.0	1.1E-10	2.2E-15	106.4	18.7	161	585-856	34-200 (200)
956	90	4LDP_B	NDP-forosamyltransferas	99.0	9.3E-11	1.9E-15	118.1	19.7	323	372-868	27-440 (455)
957	91	3Q3E_A	HMW1C-like glycosyltran	99.0	2.3E-10	4.7E-15	132.2	24.2	279	425-868	330-624 (631)
958	92	4BQE_B	ALPHA-GLUCAN PHOSPHORYL	99.0	5.5E-10	1.1E-14	136.0	28.0	315	442-868	364-865 (874)
959	93	1YGP_A	YEAST GLYCOGEN PHOSPHOR	99.0	5.2E-10	1.1E-14	136.0	27.6	304	439-868	354-872 (879)
960	94	3H4T_A	Glycosyltransferase Gtf	98.9	2.7E-10	5.5E-15	112.9	17.6	320	373-868	12-381 (404)
961	95	4REL_A	UDP-glucose:anthocyanid	98.9	3.2E-09	6.4E-14	108.3	24.5	332	378-868	21-443 (446)
962	96	4BFC_A	3-DEOXY-D-MANNO-OCTULOS	98.8	9E-10	1.8E-14	105.4	18.2	180	586-869	40-232 (235)
963	97	2F9F_A	first mannosyl transfer	98.8	9.1E-10	1.8E-14	100.5	17.2	157	582-849	18-175 (177)
964	98	5V2J_A	UDP-glycosyltransferase	98.8	4.5E-09	9.1E-14	106.2	23.7	330	376-868	20-446 (449)
965	99	5LR8_A	Hv_Pho1 (E.C.2.4.1.1);	98.8	2.8E-09	5.6E-14	130.9	25.4	241	494-868	527-917 (938)
966	100	6FJ3_A	Parathyroid hormone/par	98.8	1.5E-09	3.1E-14	121.6	20.9	174	585-868	353-532 (602)
967	101	4M83_A	Oleandomycin glycosyltr	98.8	2.1E-08	4.3E-13	103.3	25.6	318	378-868	24-398 (415)

102	1IIR_A	glycosyltransferase Gtf	98.7	2.8E-09	5.7E-14	105.8	16.5	313	373-868	12-398	(415)
103	1RRV_A	GLYCOSYLTRANSFERASE GTF	98.7	1.5E-08	3.1E-13	101.6	20.7	316	373-869	12-400	(416)
104	6IJ7_A	Rhamnosyltransferase pr	98.6	1.4E-07	2.8E-12	95.8	26.8	281	429-868	102-433	(435)
105	6BK0_A	UDP-glycosyltransferase	98.6	1.4E-07	2.8E-12	96.1	25.7	323	378-868	32-465	(467)
106	2VCH_A	HYDROQUINONE GLUCOSYLTR	98.3	7.9E-06	1.6E-10	84.3	28.7	340	373-868	18-467	(480)
107	3HBM_A	UDP-sugar hydrolase; ud	98.2	4.3E-07	8.7E-12	89.2	17.0	254	377-777	23-281	(282)
108	2PQ6_A	UDP-glucuronosyl/UDP-gl	98.0	1.6E-05	3.2E-10	81.4	22.3	333	378-868	25-477	(482)
109	2C1X_A	UDP-GLUCOSE FLAVONOID 3	97.6	0.00018	3.7E-09	74.3	21.4	284	429-868	95-450	(456)
110	5WQC_A	Orexin receptor type 2,	97.1	0.00055	1.1E-08	76.6	18.4	169	585-863	291-464	(560)
111	2O6L_B	UDP-glucuronosyltransfe	96.5	0.0036	7.2E-08	56.3	12.4	144	584-850	19-168	(170)
112	3L7I_A	Teichoic acid biosynthe	96.4	0.0077	1.6E-07	70.8	16.8	350	355-833	317-725	(729)
113	5U09_A	Cannabinoid receptor 1,	96.0	0.044	8.8E-07	61.4	18.2	177	585-870	243-424	(508)
114	5ZIC_A	Alpha-1,6-mannosylglyco	95.9	0.014	2.8E-07	69.0	13.7	157	585-873	226-407	(523)
115	1PSW_A	ADP-HEPTOSE LPS HEPTOSY	95.3	0.13	2.6E-06	52.7	14.8	166	585-831	179-348	(348)
116	5GVV_A	Glycosyl transferase fa	95.3	0.023	4.6E-07	62.2	9.9	111	606-778	289-401	(406)
117	2GT1_A	Lipopolysaccharide hept	94.9	0.16	3.3E-06	51.5	13.4	145	585-831	177-325	(326)
118	3TOV_B	Glycosyl transferase fa	94.4	0.24	4.8E-06	50.6	12.3	113	585-760	184-299	(349)
119	6JTD_A	C-glycosyltransferase;	92.6	1.7	3.5E-05	46.2	14.0	166	585-868	273-476	(483)
120	5NLM_B	indoxyl UDP-glucosyltra	90.1	8.9	0.00018	40.9	15.2	167	585-868	273-474	(478)
121	6MGB_A	Capsular polysaccharide	87.7	4.1	8.4E-05	43.9	10.4	102	584-746	153-262	(326)
122	5IJO_T	Nuclear pore complex pr	85.2	31	0.00064	41.9	16.5	192	129-377	322-515	(522)
123	6HLP_A	Substance-P receptor,Su	84.5	21	0.00043	40.1	13.9	177	585-870	256-437	(520)
124	6MGC_A	Capsule polysaccharide	83.7	5.7	0.00012	43.7	8.9	101	585-746	147-255	(361)
125	1JIX_A	DNA BETA-GLUCOSYLTRANSF	76.1	8.9	0.00018	43.9	6.9	108	696-855	229-345	(351)
126	6MGD_A	Capsular polysaccharide	66.3	30	0.00061	37.7	7.9	99	585-746	151-259	(332)
127	4RAP_I	Glycosyltransferase Tib	57.6	2.3E+02	0.0047	31.7	12.8	169	585-828	215-389	(406)
128	5IJO_G	Nuclear pore complex pr	57.6	1.2E+02	0.0024	37.8	11.3	178	121-308	241-431	(599)
129	5FA1_A	Cell division protein Z	56.1	57	0.0012	37.3	8.0	91	585-746	219-316	(410)
130	2JZC_A	UDP-N-acetylglucosamine	53.1	2.4E+02	0.0049	30.3	11.5	120	568-748	10-160	(224)
131	4UXV_A	SEPTATION RING FORMATIO	50.5	5.5E+02	0.011	29.9	14.6	150	138-328	361-515	(545)
132	2KS6_A	UDP-N-acetylglucosamine	49.7	1.8E+02	0.0036	30.6	9.6	108	582-750	1-139	(201)
133	5XEI_A	Chromosome partition pr	43.5	7.5E+02	0.015	28.8	21.8	316	136-481	161-482	(540)
134	5ZIB_A	Alpha-1,6-mannosylglyco	42.1	54	0.0011	40.7	5.1	49	697-748	374-423	(626)
135	4P5E_B	2'-deoxynucleoside 5'-p	36.7	3.1E+02	0.0063	25.7	8.2	80	625-746	1-99	(152)
136	5NPS_A	UDP-N-acetylglucosamine	35.2	1.7E+02	0.0034	37.3	7.7	105	590-749	519-625	(718)
137	6QAI_B	deoxyribosyltransferase	34.6	5.5E+02	0.011	24.5	10.1	83	624-746	3-99	(156)

138	3EHD_A	uncharacterized conserv	33.2	4.8E+02	0.0097	24.8	9.0	82	624-746	2-102	(162)
139	4UX3_A	STRUCTURAL MAINTENANCE	32.9	1.2E+03	0.025	28.0	22.5	328	128-482	140-492	(543)
140	6EK8_A	YaxB; pathogens, pore f	25.7	8.4E+02	0.017	27.8	10.6	107	138-244	147-255	(344)
141	6CFZ_H	Ask1, Dad3, Dad2, Duo1,	25.4	1.3E+02	0.0027	26.3	3.4	35	273-308	8-42	(56)
142	5AX7_A	Pyruvyl transferase 1;	23.8	1.3E+03	0.026	25.1	18.0	227	414-746	68-300	(348)
143	3U4Q_B	ATP-dependent helicase/	22.8	1.9E+03	0.039	27.8	13.8	205	215-429	383-615	(1166)
144	3ILW_A	DNA gyrase subunit A (E	21.2	1E+03	0.02	28.1	10.4	155	232-392	298-463	(470)
145	5J0J_A	designed protein 2L6HC3	21.0	7.8E+02	0.016	22.7	7.2	68	139-217	9-76	(79)
146	2KE4_A	Cdc42-interacting prote	20.2	9.1E+02	0.018	22.6	8.0	79	147-225	13-91	(98)